Calibrated radar observations of the equatorial mesosphere and ionosphere during an 11-day campaign

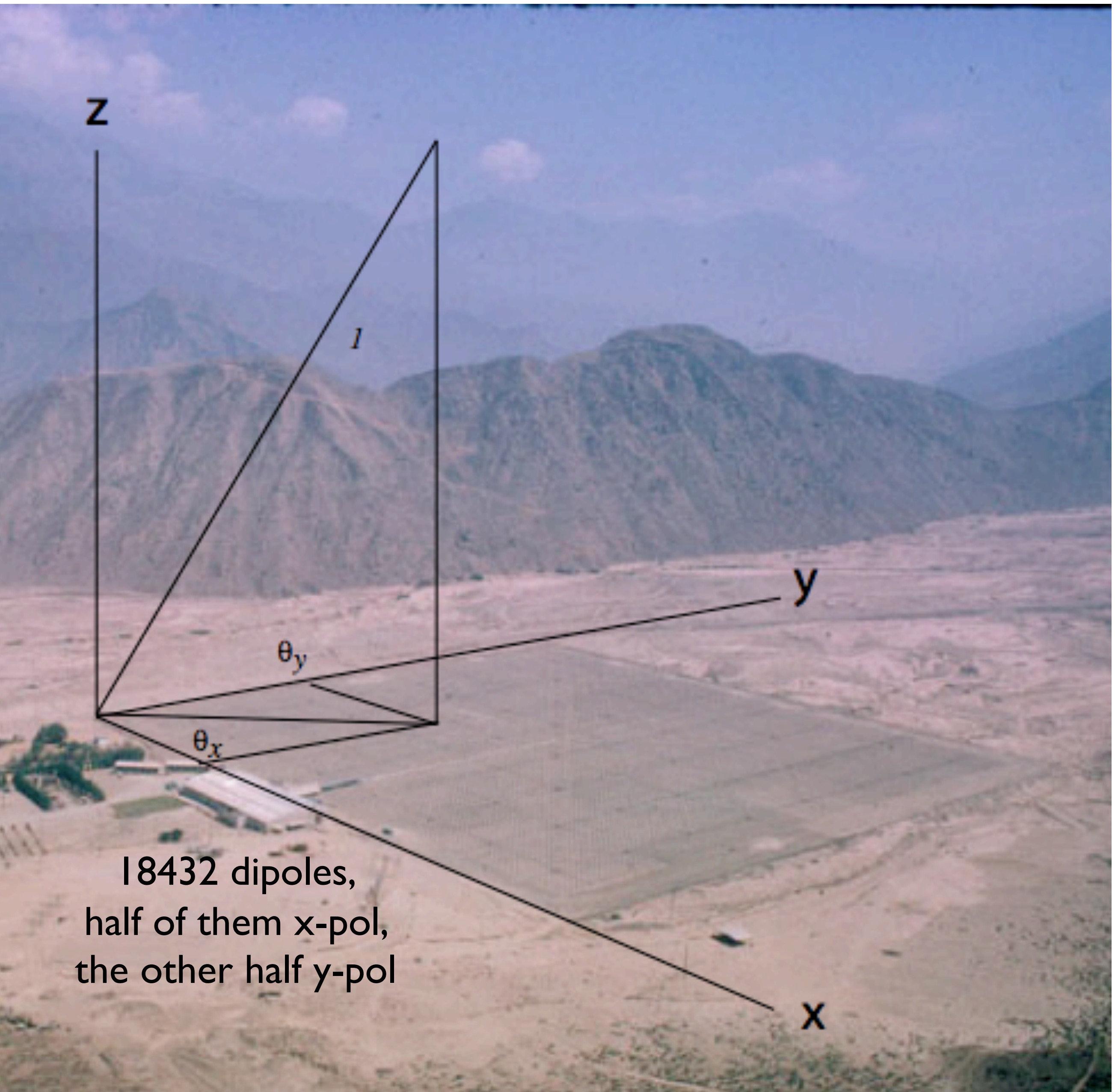

E. Kudeki[1], M. Milla[1], P. Reyes[1],

G. Lehmacher[2],

J. L. Chau[3], K. M. Kuyeng[3],
C.DeLaJara[3]

(1) University of Illinois
(2) Clemson University
(3) Jicamarca Radio Observatory

In Jicamarca MST experiments we have been (since 1985) recording F-region incoherent scatter returns to calibrate the MST data for absolute radar cross-section (RCS) measurements (without keeping track of system parameters).

OUTLINE:

1) Describe how we do the calibrations, and
2) Show examples with data collected during an 11-day run that took place in Jan 2009.

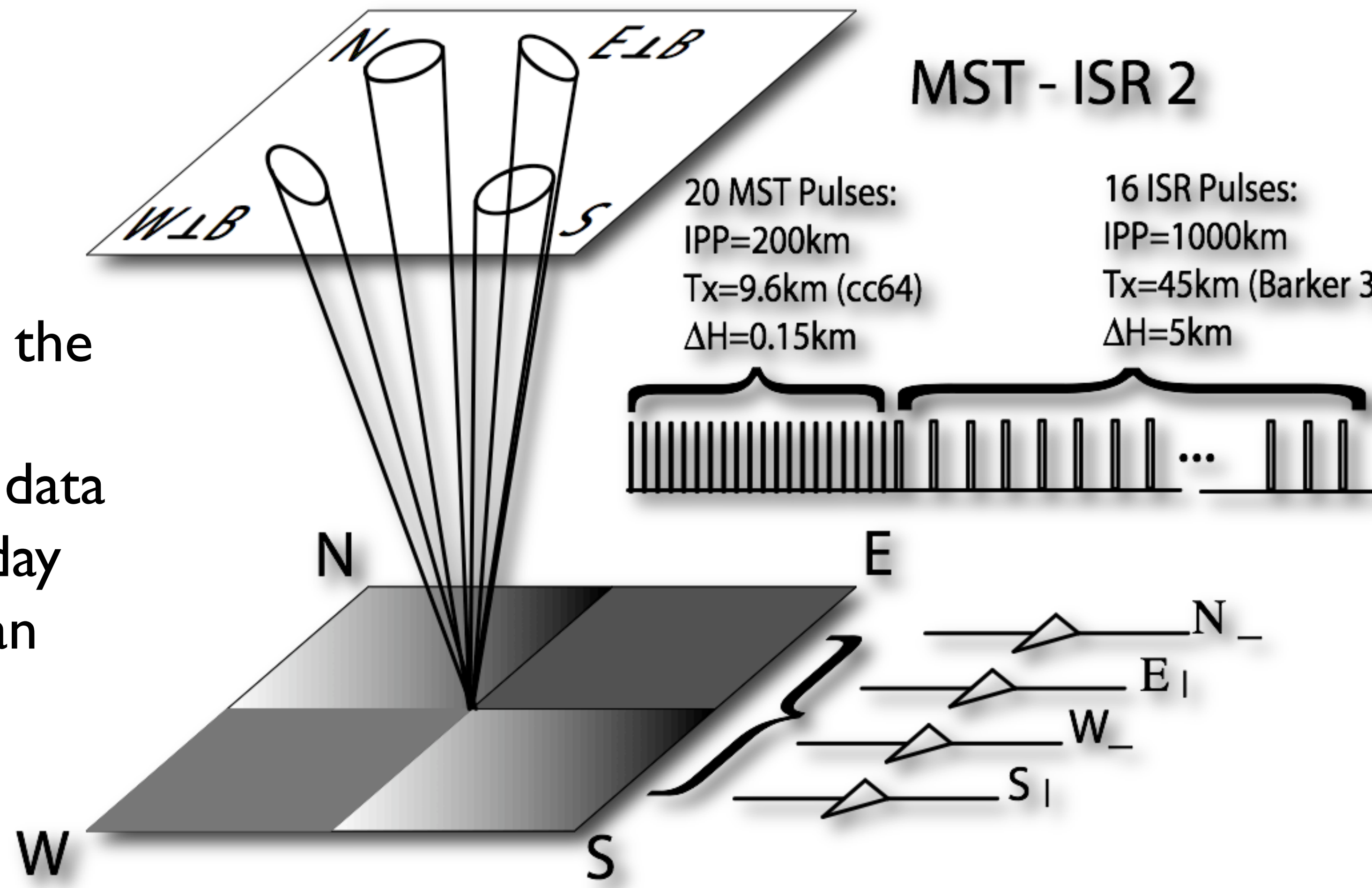

Absolute RCS measurements can be done by comparing the scattered power from the MST region with F-region ISR power, because ISR power is proportional to F-region electron density which can be independently measured (or guessed).

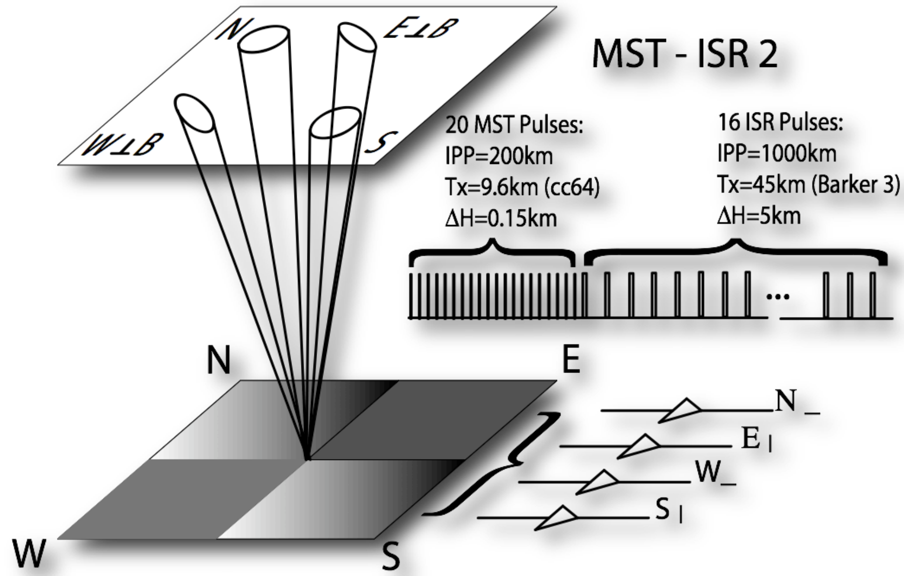

But there are complications:

1) The proportionality factor depends on Te/Ti (a minor effect)

2) Unless a magneto-ionic "normal mode" is used for tx and rx, there will be **magneto-ionic power distortions** --- wiggles --- in ISR profiles to account for.

In the original **single beam** MST experiment of **Woodman and Guillen (1974)** a circular polarized normal mode was used and calibrated results were discussed.

But when JRO started the 4-beam **wind profiling** experiments **with linear polarized antennas** (unavoidable), the practice of maintaining calibrated operations was lost.

Only 2 polarizations are available for 4 beams!

x-pol (D-pol) excites and detects the North and West beams

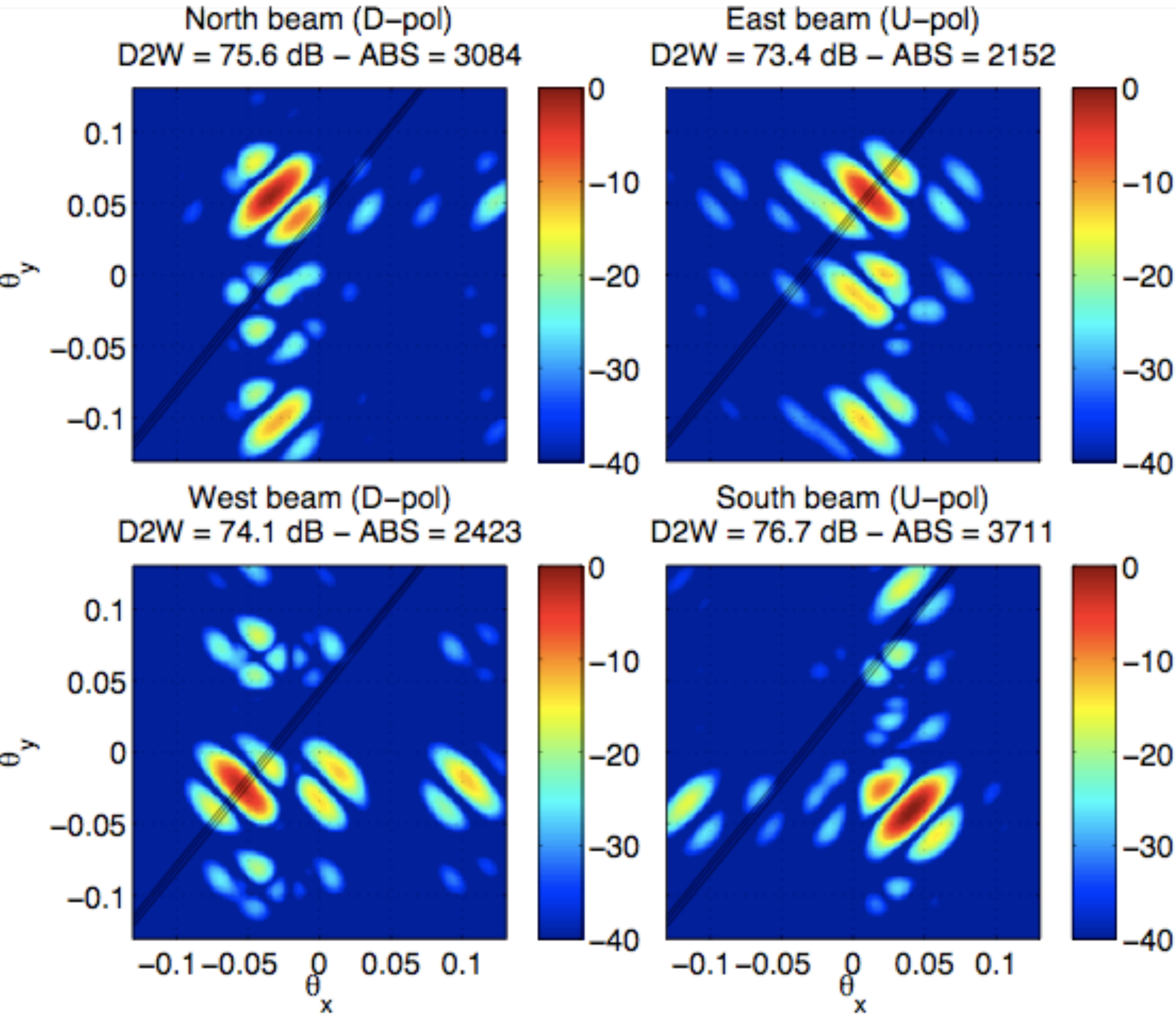

y-pol (U-pol) is used for East and South beams

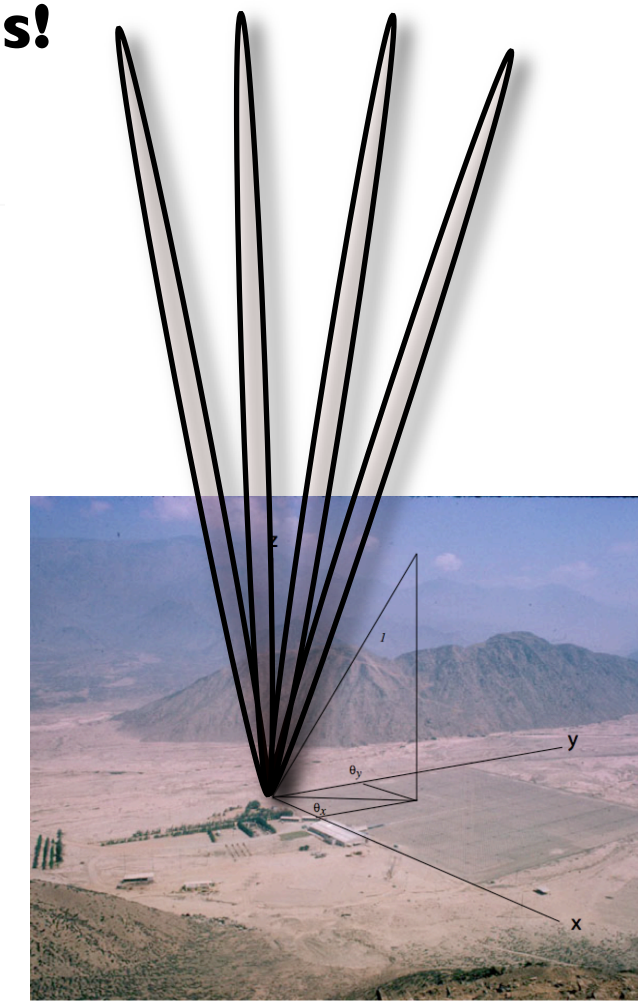

But magneto-ionic distortions (see next) cross-couple the beams because different beams have different aspect angles to **B**

~perp to B,
Cotton-Mouton effect,
linear normal modes

~2 deg off perp,
Faraday rotation,
~circular norma
modes

as the wave propagates wave polarization is modified

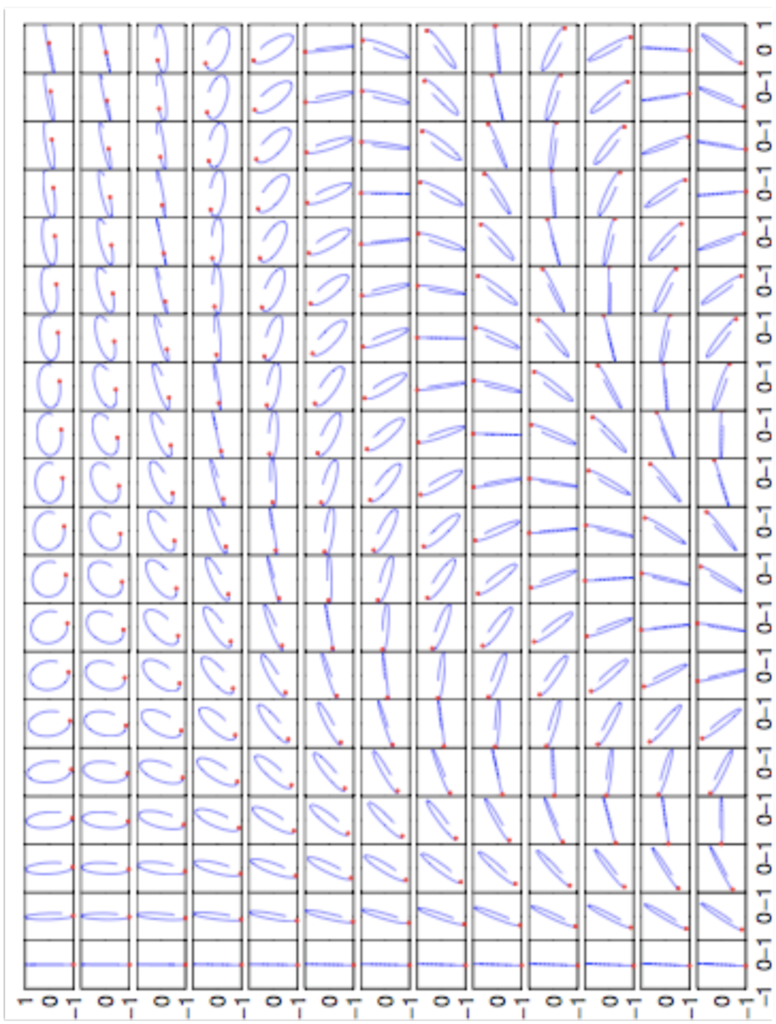

2-way beam patterns:

x (D) -pol

y (U) -pol

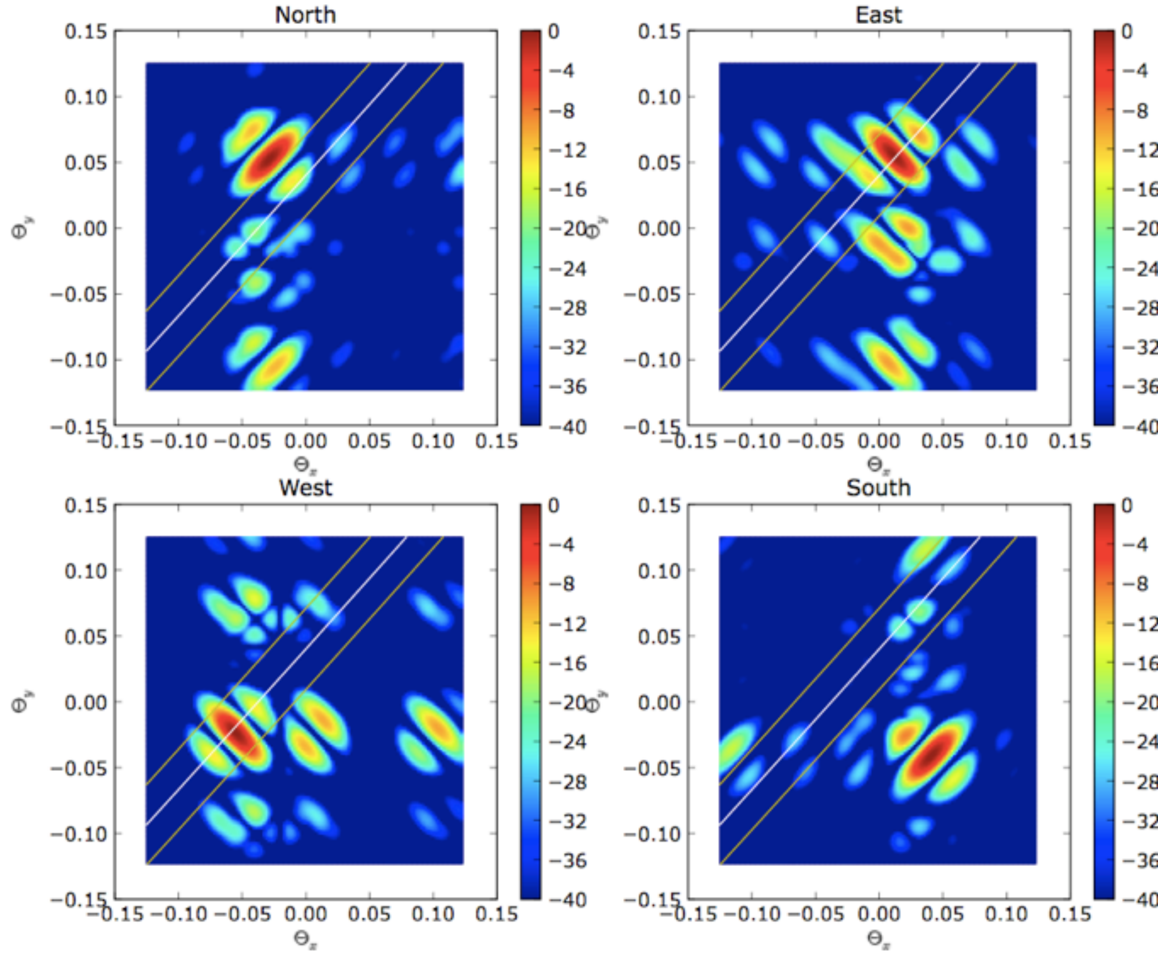

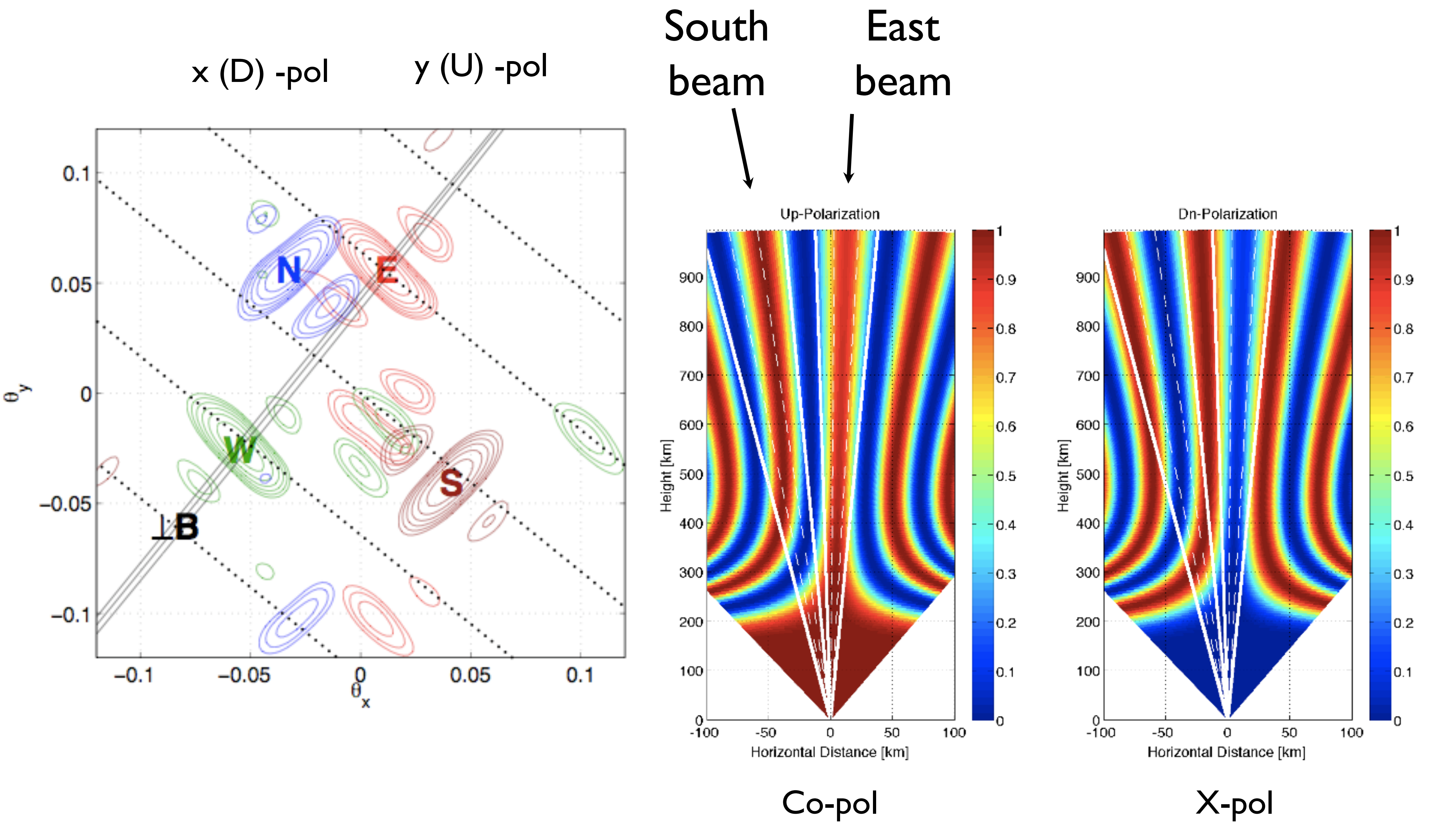

East Beam perp-to-B suffers less “Faraday rotation” than the off perpendicular South Beam that “loses” a lot of power (to sidelobes of X-pol beams).

Examples of how power varies with height in different beams will follow...

but first, here is an example of high-resolution MST-mode data:

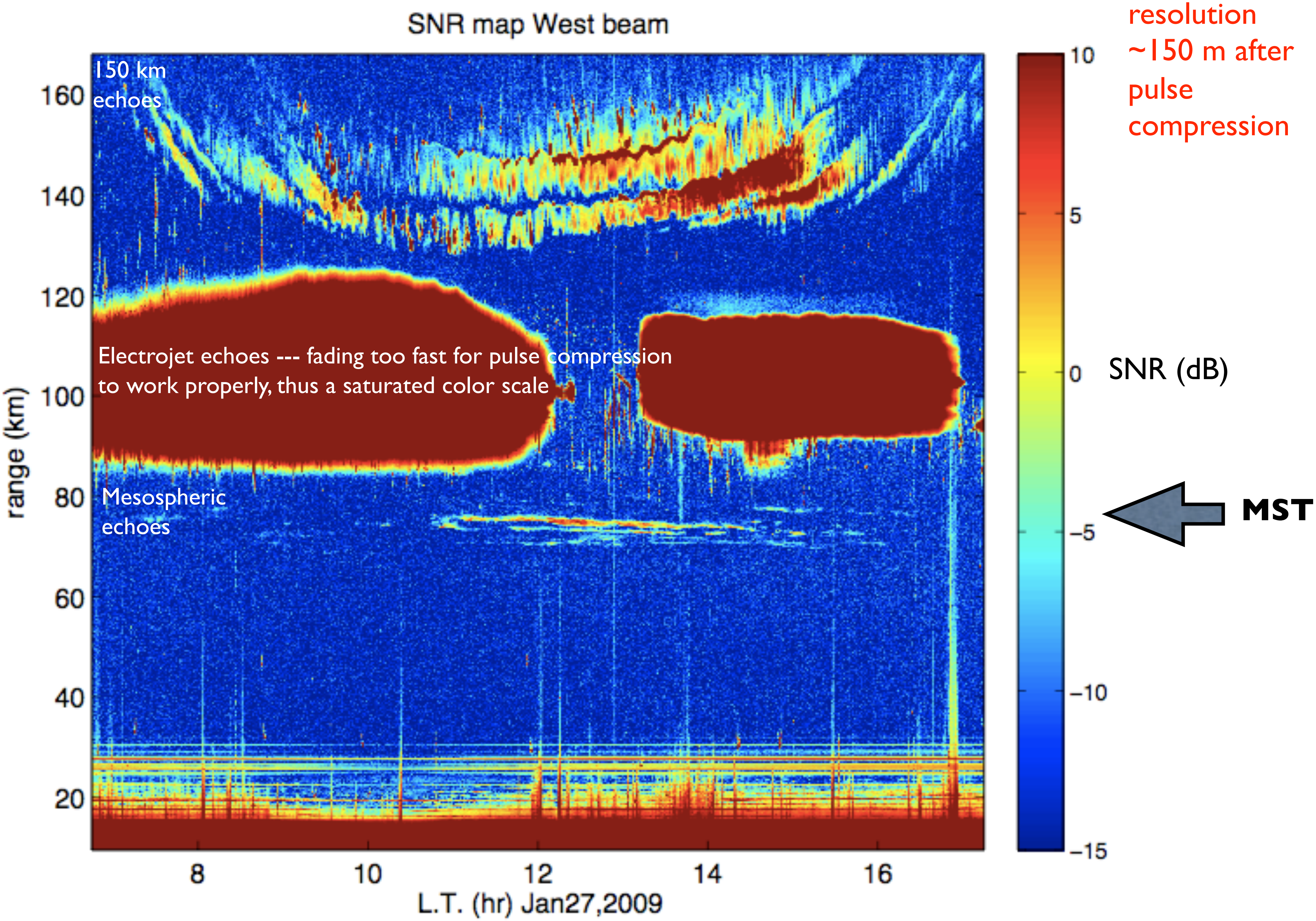

Height resolution ~150 m after pulse compression

Jan 23, 2009

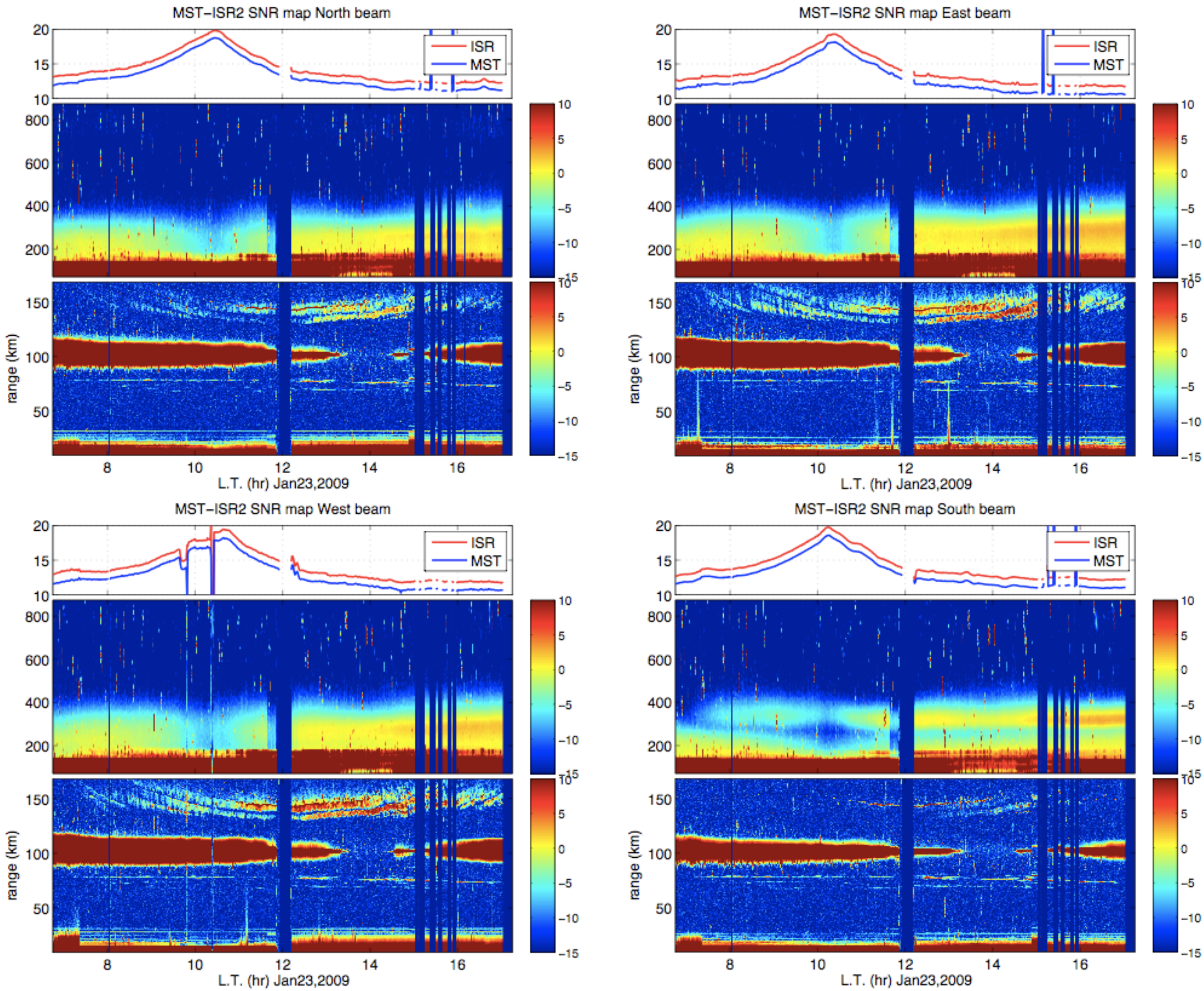

MST−ISR2 SNR map North beam
ISR
MST
range (km)
L.T. (hr) Jan23,2009
MST−ISR2 SNR map East beam
ISR
MST
range (km)
L.T. (hr) Jan23,2009
MST−ISR2 SNR map West beam
ISR
MST
range (km)
L.T. (hr) Jan23,2009
MST−ISR2 SNR map South beam
ISR
MST
range (km)
L.T. (hr) Jan23,2009

MST and *ISR* mode data from Jan 2005 --- pronounced South Beam wiggles...

N

weaker Faraday wiggles

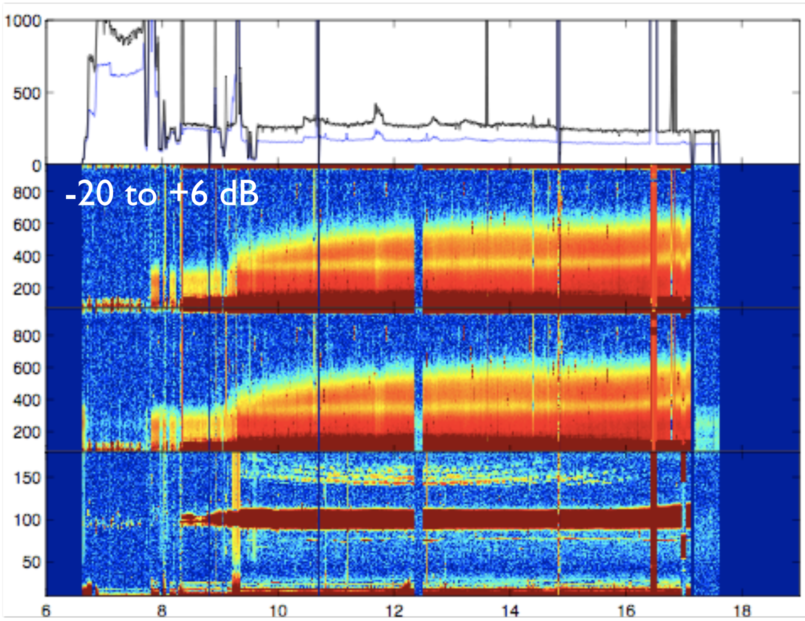

E

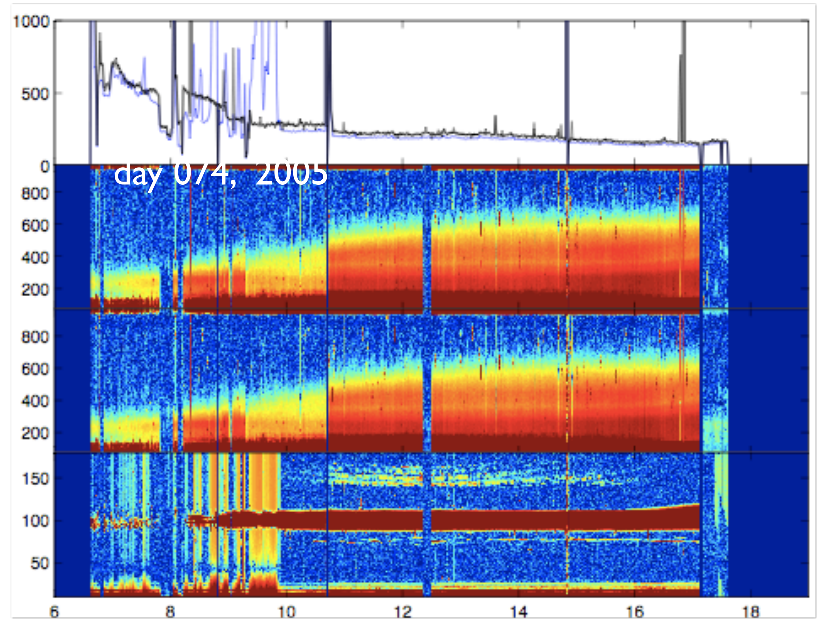

Interference, T/R switch, and sychro problems

W

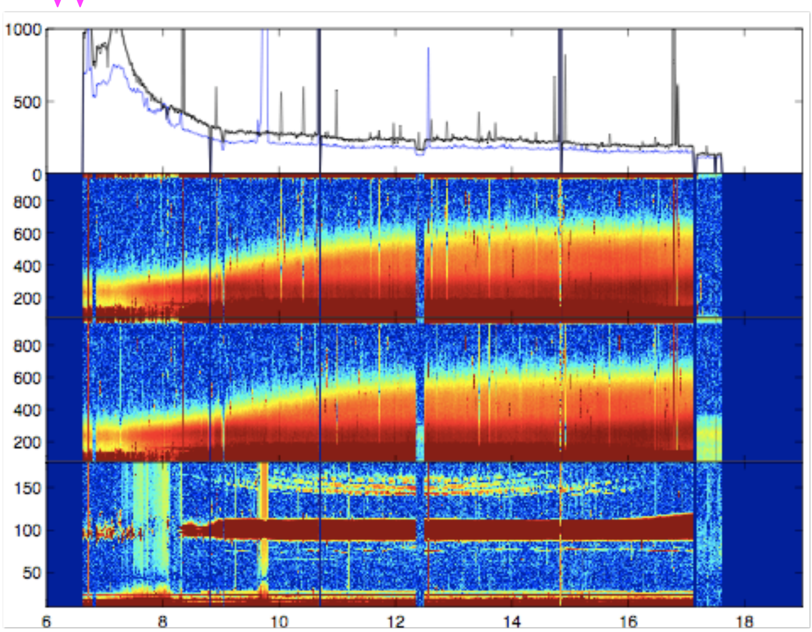

S

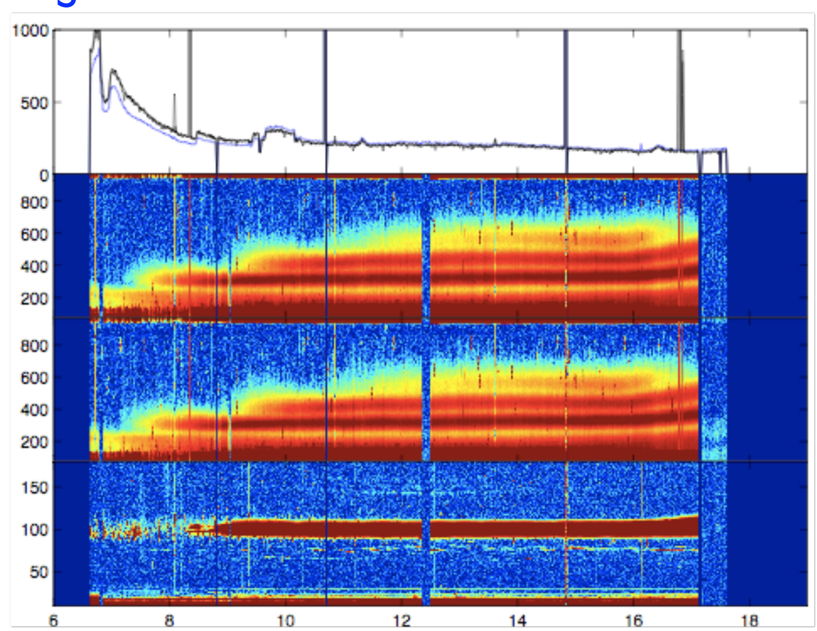

Faraday like wiggles on S

Fit the observed ISR power profiles to density dependent model equations like

$$\langle |V_r(t)|^2 \rangle = \frac{\kappa}{r^2} \int d\Omega \, G_{tx} G_{rx} \, \tilde{\sigma}$$

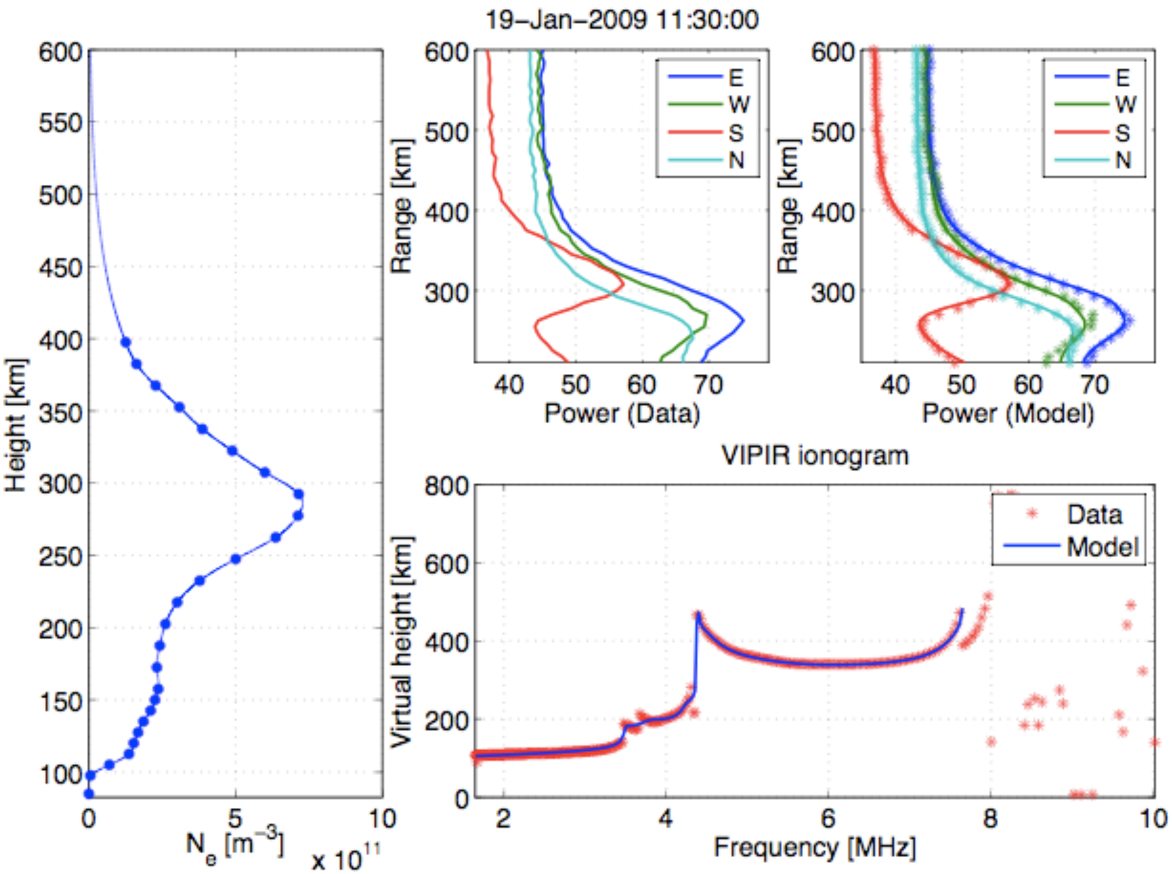

and estimate the "calibration constants"

$$\kappa \propto \frac{E_t \delta r}{L}$$

one for each beam.

Forward model details...

A magneto-ionic propagation problem through a multi-slab ionosphere model:

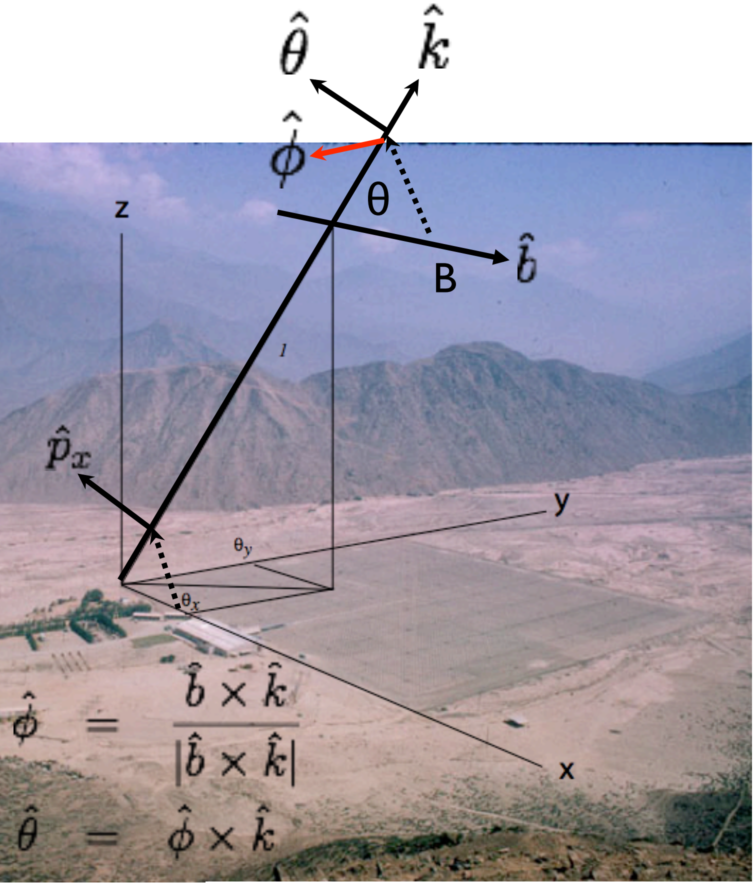

Polarization unit vector: $\hat{p}_x = \frac{\hat{k} \times \hat{k} \times \hat{x}}{|\hat{k} \times \hat{k} \times \hat{x}|} \equiv E_{xo}\hat{x} + E_{yo}\hat{y} + E_{zo}\hat{z} \equiv E_{\theta o}\hat{\theta} + E_{\phi o}\hat{\phi}$

$$Y_L = Y\cos\theta, \quad Y_T = Y\sin\theta, \quad Y = \frac{\Omega}{\omega}, \quad X = \frac{\omega_p^2}{\omega^2}$$

$$F_O = F_1 - F_2, \quad F_X = F_1 + F_2, \quad F_1 = \frac{Y_T^2/2}{1-X}, \quad F_2^2 = F_1^2 + Y_L^2$$

$$n_{O,X}^2 = 1 - \frac{X}{1 - F_{O,X}}$$

$$\Delta n = \frac{n_O - n_X}{2} \qquad \bar{n} = \frac{n_O + n_X}{2} \qquad a = \frac{F_O}{Y_L}$$

$$\mathbf{E}(\delta r) = \begin{bmatrix} E_\theta \\ E_\phi \end{bmatrix} = \underbrace{\frac{e^{-jk\bar{n}\delta r}}{1+a^2}\begin{bmatrix} a^2 e^{jk\Delta n\delta r} + e^{-jk\Delta n\delta r} & 2a\sin(k\Delta n\delta r) \\ -2a\sin(k\Delta n\delta r) & a^2 e^{-jk\Delta n\delta r} + e^{jk\Delta n\delta r} \end{bmatrix}}_{\bar{\bar{M}}} \begin{bmatrix} E_{\theta_o} \\ E_{\phi_o} \end{bmatrix}$$

Iterate after modifying $\Delta n, \bar{n}, a, \hat{\theta}, \hat{\phi}$ due to slow varing density and $\vec{B}$

$$v_x \propto \hat{p}_x \cdot (E_\theta\hat{\theta} + E_\phi\hat{\phi}) \qquad v_y \propto \hat{p}_y \cdot (E_\theta\hat{\theta} + E_\phi\hat{\phi})$$

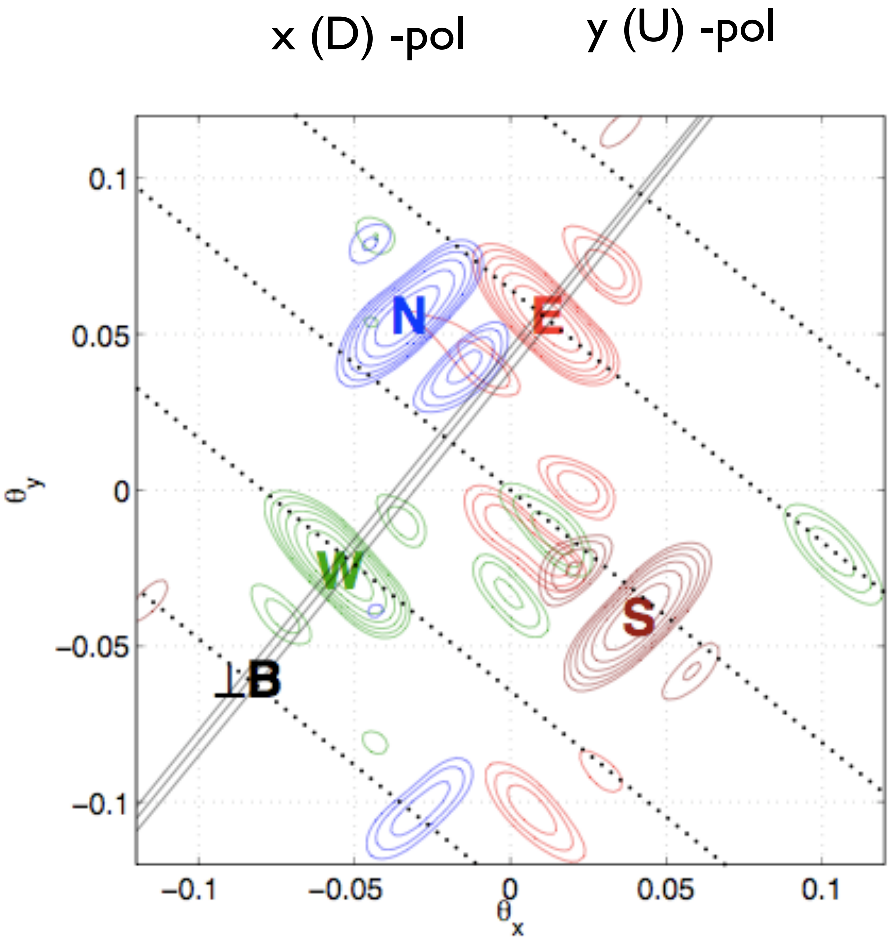

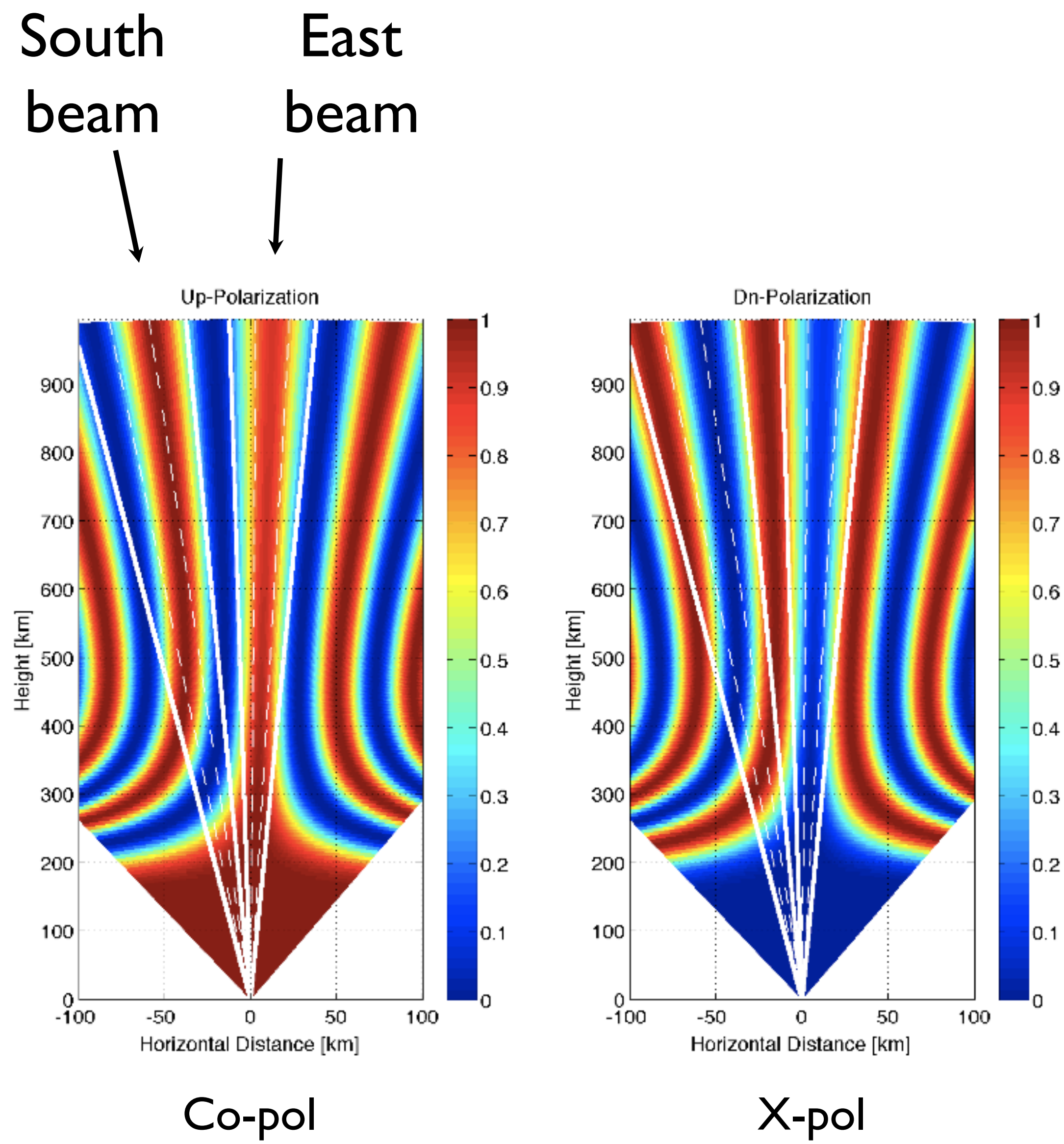

These factors are subsequently beam and electron density weighted and added over all angles to get the simulated power profiles.

One more complication: dependence of cross-section on Te/Ti

166 14. RADIO WAVE SCATTERING FROM THE IONOSPHERE

$f(\frac{T_e}{T_i})$

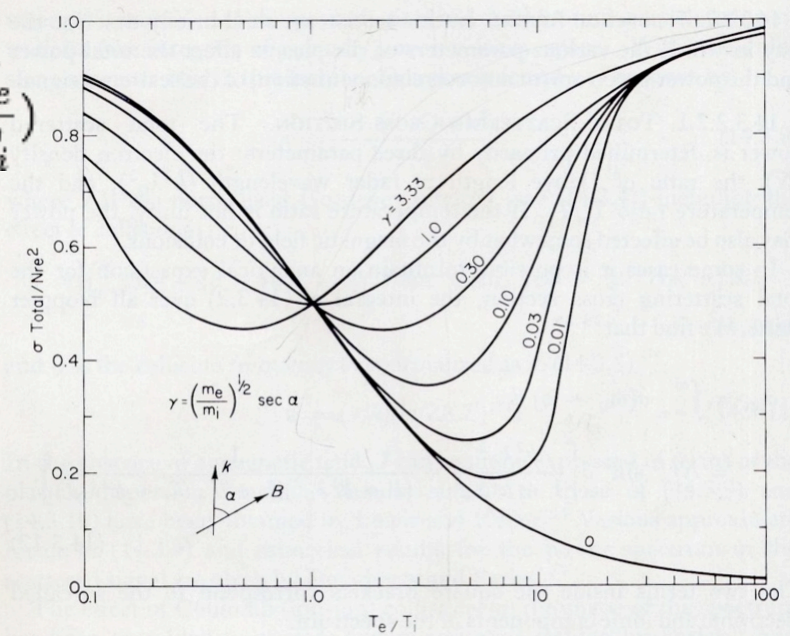

FIG. 7. The dependence of the scattering cross section for incoherent scatter on the electron-to-ion temperature ratio and $\gamma = (m_e/m_i)^{1/2} \sec\alpha$, where α is the angle between **k** and the magnetic field **B**, and $(m_e/m_i)^{1/2} \approx 6 \times 10^{-3}$ in the *F* region. The Debye length is assumed to be negligibly small. The curve for $\gamma = 0$ is just $(1 + T_e/T_i)^{-1}$. [From D. T. Farley, *J. Geophys. Res.* **71**, 4091 (1966).]

$$\tilde{\sigma} = 4\pi r_e^2 N_e f(\frac{T_e}{T_i})$$

$f(\frac{T_e}{T_i})$

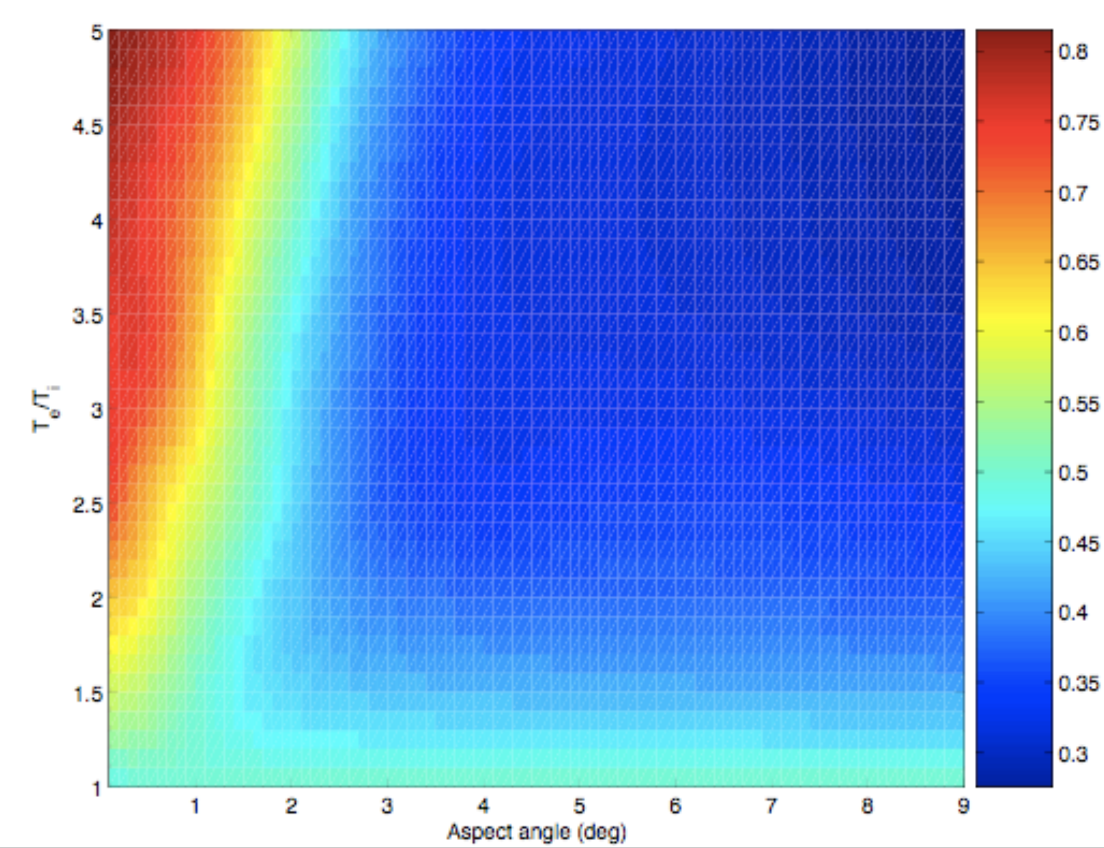

Fit the ISR power profile data *from all four beams* to power profile model

$$\langle |V_r(t)|^2 \rangle = \frac{\kappa}{r^2} \int d\Omega \, G_{tx} G_{rx} \, \tilde{\sigma}$$

and estimate density and Te/Ti profiles and calibration constants

$$\kappa = \frac{E_t \lambda^2 \langle |N_r(t)|^2 \rangle \delta r}{(4\pi)^3 \frac{1}{2} k_B T_a L}$$

ISR power data

Model fits

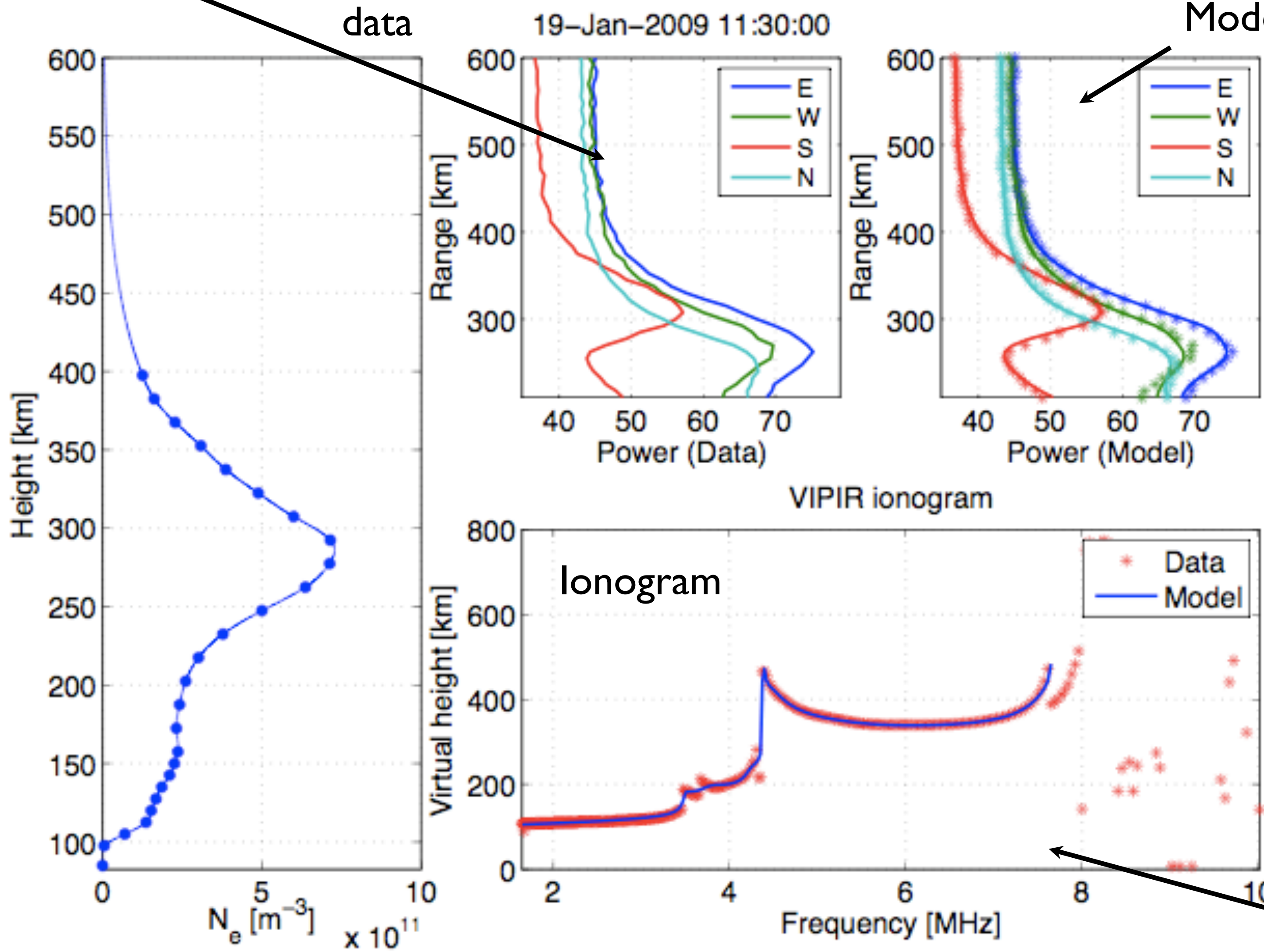

Density estimate

Useful for “reality check”, but not essential for obtaining reasonable fits

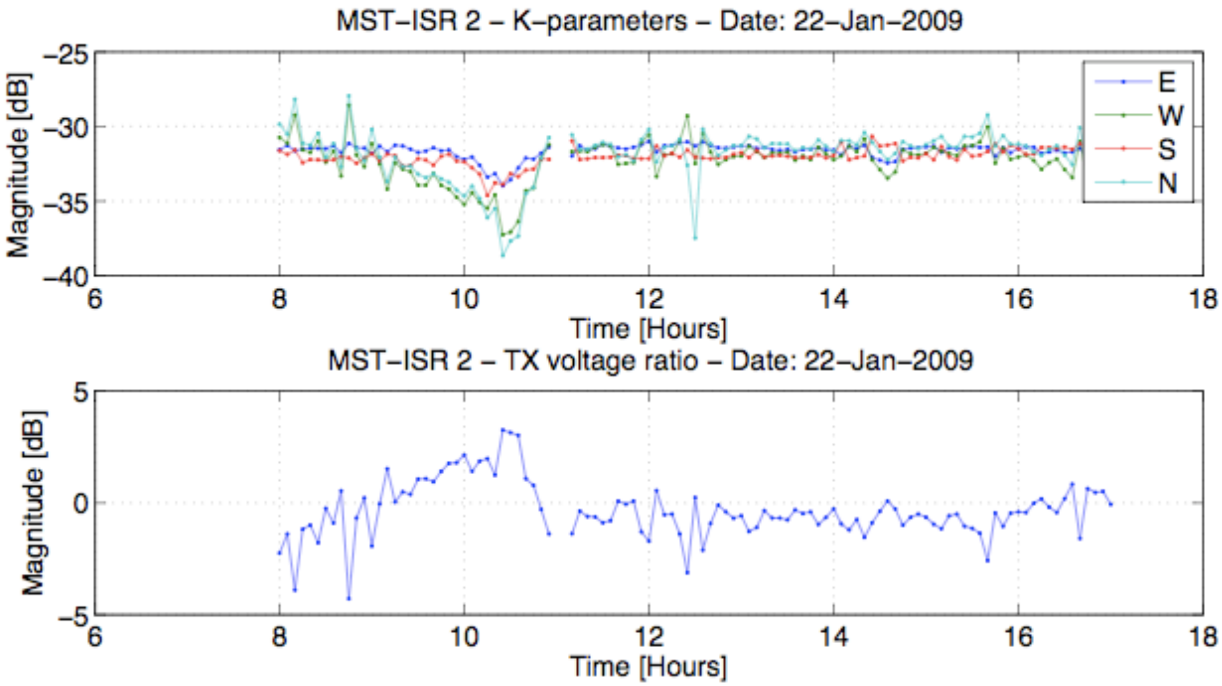
MST–ISR 2 – K–parameters – Date: 22–Jan–2009
Magnitude [dB]
Time [Hours]
E
W
S
N
MST–ISR 2 – TX voltage ratio – Date: 22–Jan–2009
Magnitude [dB]
Time [Hours]

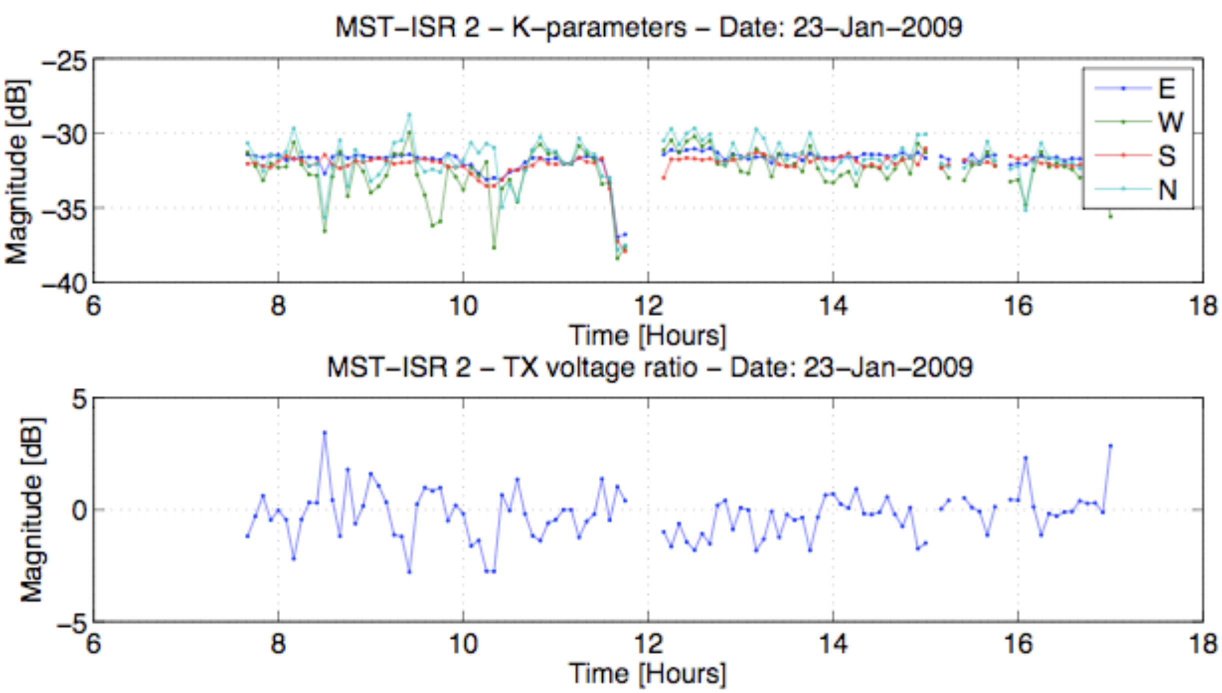
MST–ISR 2 – K–parameters – Date: 23–Jan–2009
Magnitude [dB]
Time [Hours]
E
W
S
N
MST–ISR 2 – TX voltage ratio – Date: 23–Jan–2009
Magnitude [dB]
Time [Hours]

Procedure summary:

Fit the ISR power profile data *from all four beams* to power profile model

$$\langle |V_r(t)|^2 \rangle = \frac{\kappa}{r^2} \int d\Omega \, G_{tx} G_{rx} \, \tilde{\sigma}$$

and estimate density and Te/Ti profiles and calibration constants for each radar beam

$$\kappa = \frac{E_t \lambda^2 \langle |N_r(t)|^2 \rangle \delta r}{(4\pi)^3 \frac{1}{2} k_B T_a L}$$

Estimate D-region cross-sections using

$$\tilde{\sigma}_D = \frac{r^2 \langle |V_r(t)|^2 \rangle_D}{\kappa_D \int d\Omega \, G_{tx} G_{rx}}$$

with D-region power data and rescaled calibration constants

$$\kappa_D = \kappa \frac{E_D \langle |N_r(t)|^2 \rangle_D \delta r_D}{E_F \langle |N_r(t)|^2 \rangle_F \delta r_F}$$

$$\frac{E_D}{E_F} = \frac{\tau_D}{\tau_F} = \frac{9.6 \text{ km } \times 20}{9.6 \text{ km } \times 5} = 4 \qquad \frac{\langle |N_r(t)|^2 \rangle_D}{\langle |N_r(t)|^2 \rangle_F} \sim 1 \qquad \frac{\delta r_D}{\delta r_F} \sim \frac{0.15 \text{ km}}{15 \text{ km}} = 10^{-2}$$

Obtain D-region cross-section estimates in terms of an “equivalent” because of the way the fitting is done

$$X = \frac{\omega_p^2}{\omega^2} \sim \frac{80.6N}{f^2}$$

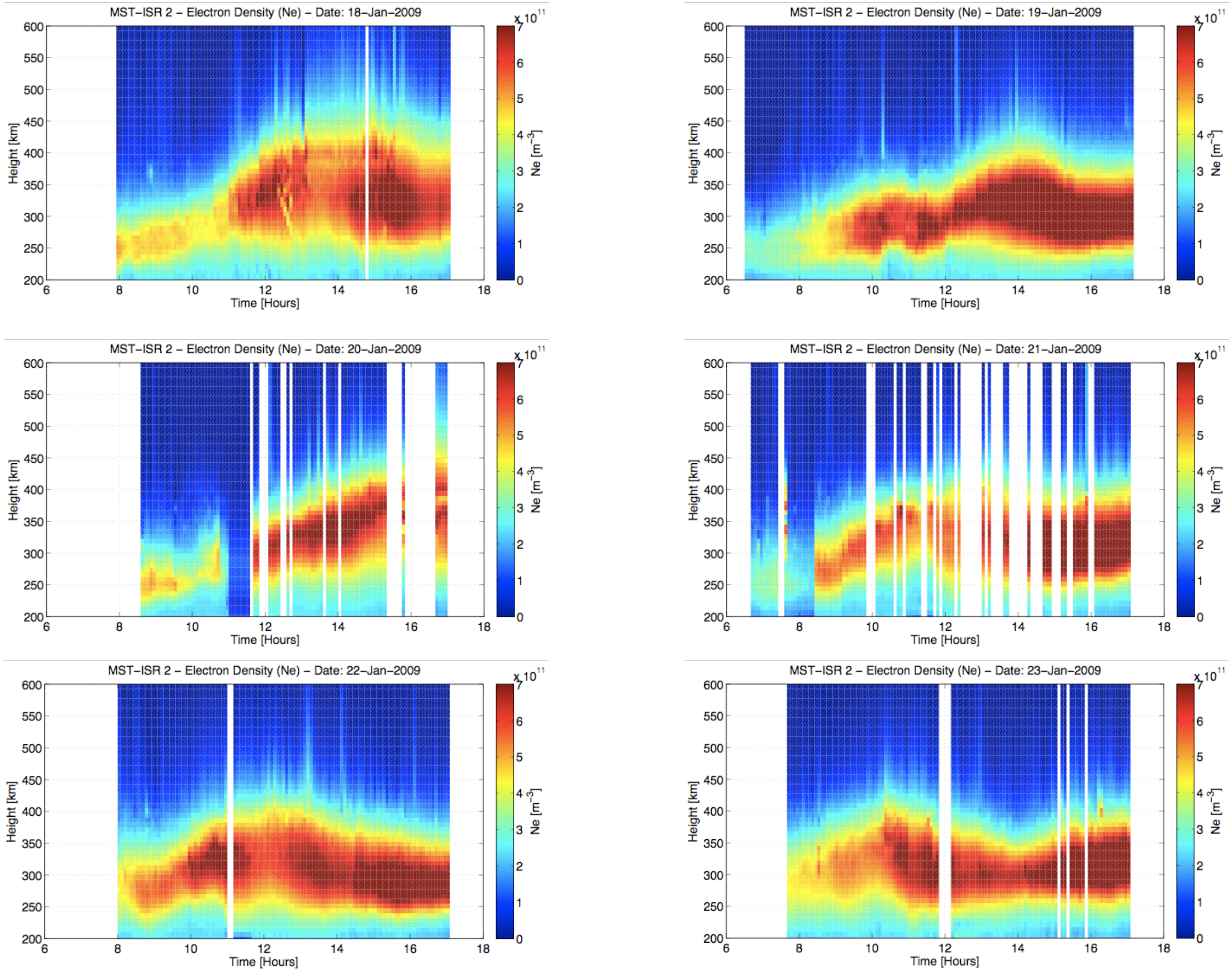
MST–ISR 2 – Electron Density (Ne) – Date: 18–Jan–2009
MST–ISR 2 – Electron Density (Ne) – Date: 19–Jan–2009
MST–ISR 2 – Electron Density (Ne) – Date: 20–Jan–2009
MST–ISR 2 – Electron Density (Ne) – Date: 21–Jan–2009
MST–ISR 2 – Electron Density (Ne) – Date: 22–Jan–2009
MST–ISR 2 – Electron Density (Ne) – Date: 23–Jan–2009
Height [km]
Time [Hours]
Ne [m^{-3}]
x 10^{11}

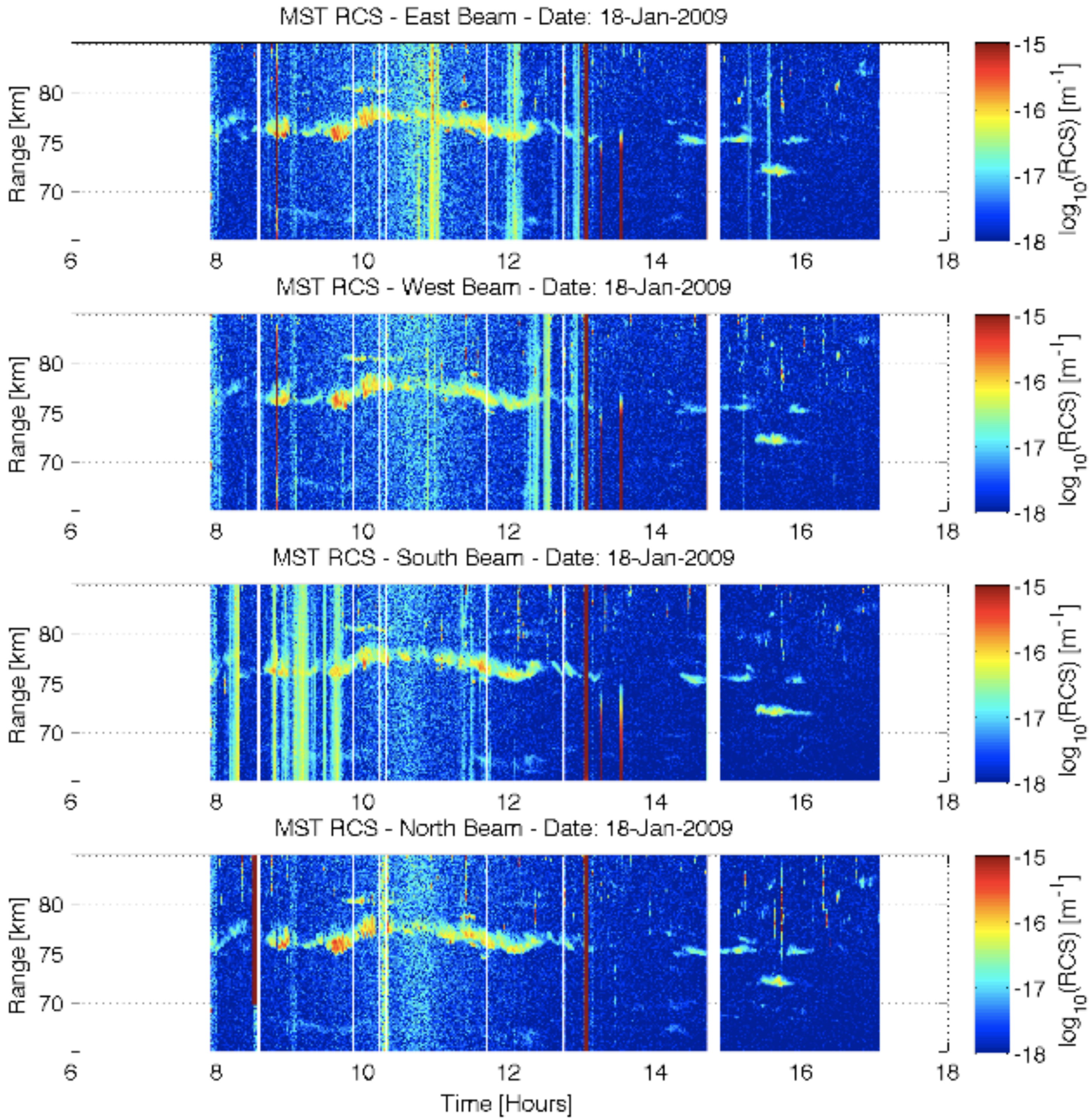

MST RCS - East Beam - Date: 18-Jan-2009
MST RCS - West Beam - Date: 18-Jan-2009
MST RCS - South Beam - Date: 18-Jan-2009
MST RCS - North Beam - Date: 18-Jan-2009
Range [km]
70
75
80
6
8
10
12
14
16
18
Time [Hours]
log10(RCS) [m-1]
-15
-16
-17
-18

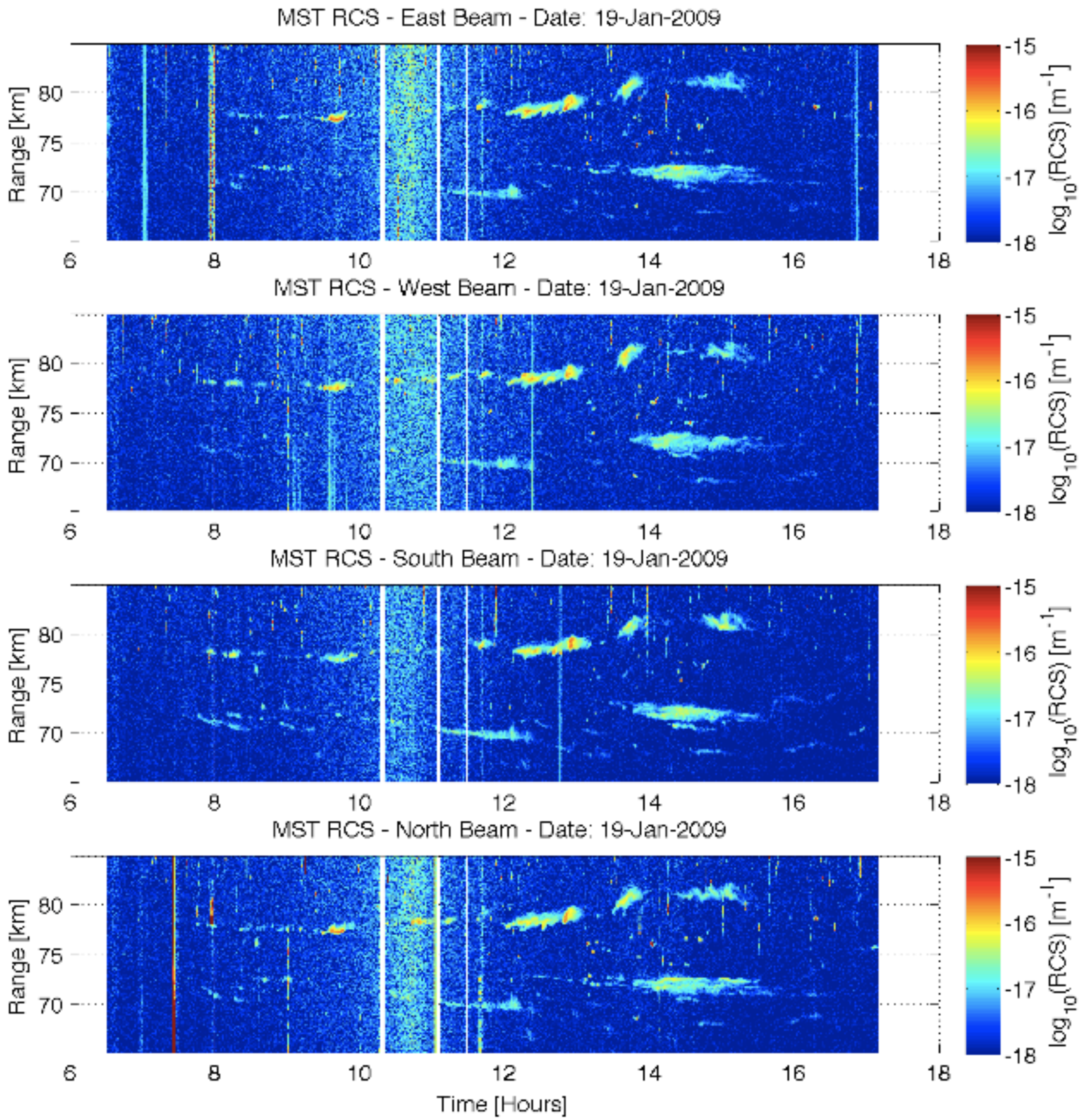
MST RCS - East Beam - Date: 19-Jan-2009
MST RCS - West Beam - Date: 19-Jan-2009
MST RCS - South Beam - Date: 19-Jan-2009
MST RCS - North Beam - Date: 19-Jan-2009
Range [km]
70
75
80
6
8
10
12
14
16
18
Time [Hours]
log10(RCS) [m-1]
-15
-16
-17
-18

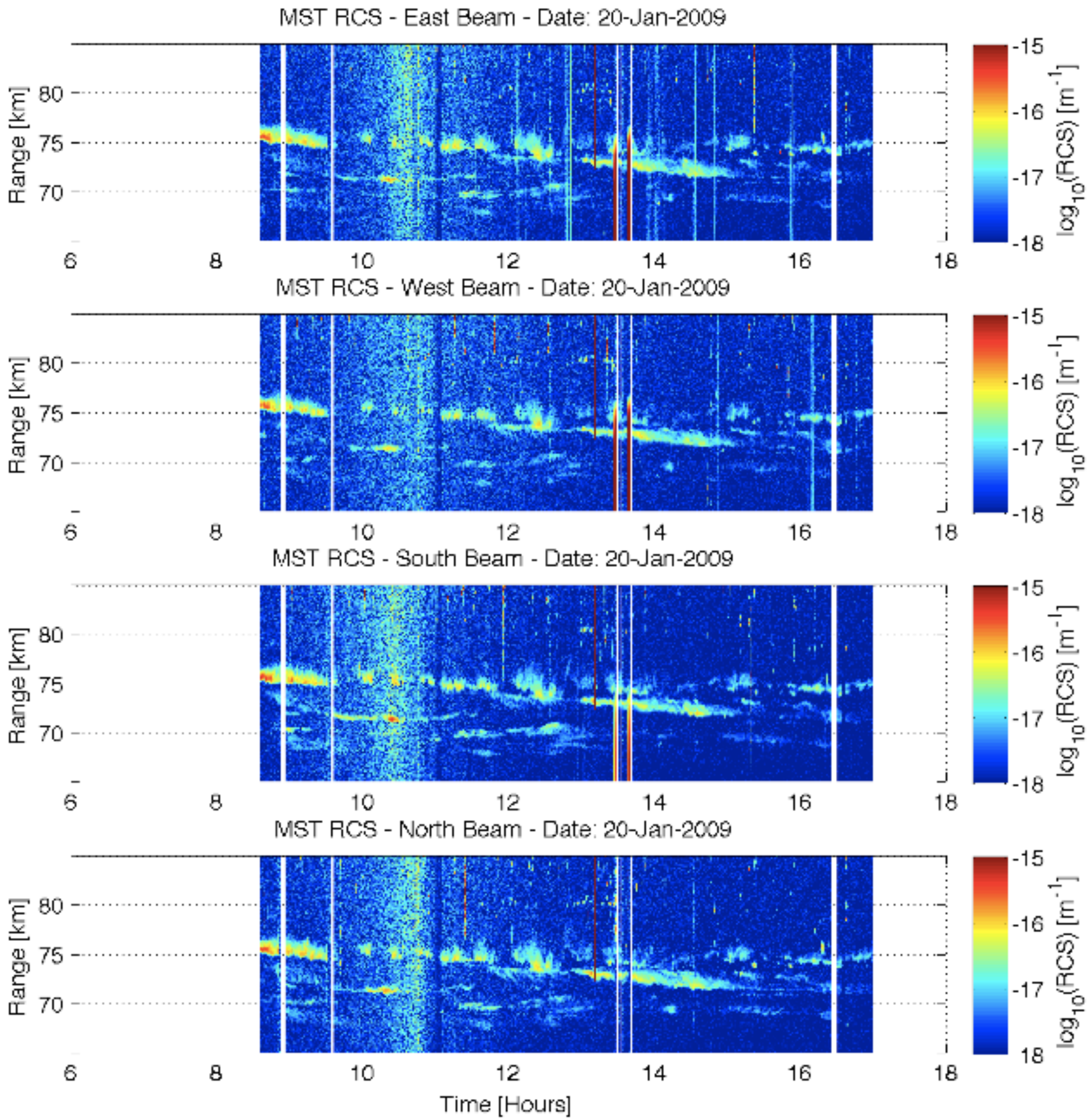
MST RCS - East Beam - Date: 20-Jan-2009
MST RCS - West Beam - Date: 20-Jan-2009
MST RCS - South Beam - Date: 20-Jan-2009
MST RCS - North Beam - Date: 20-Jan-2009
Range [km]
Time [Hours]
log10(RCS) [m-1]

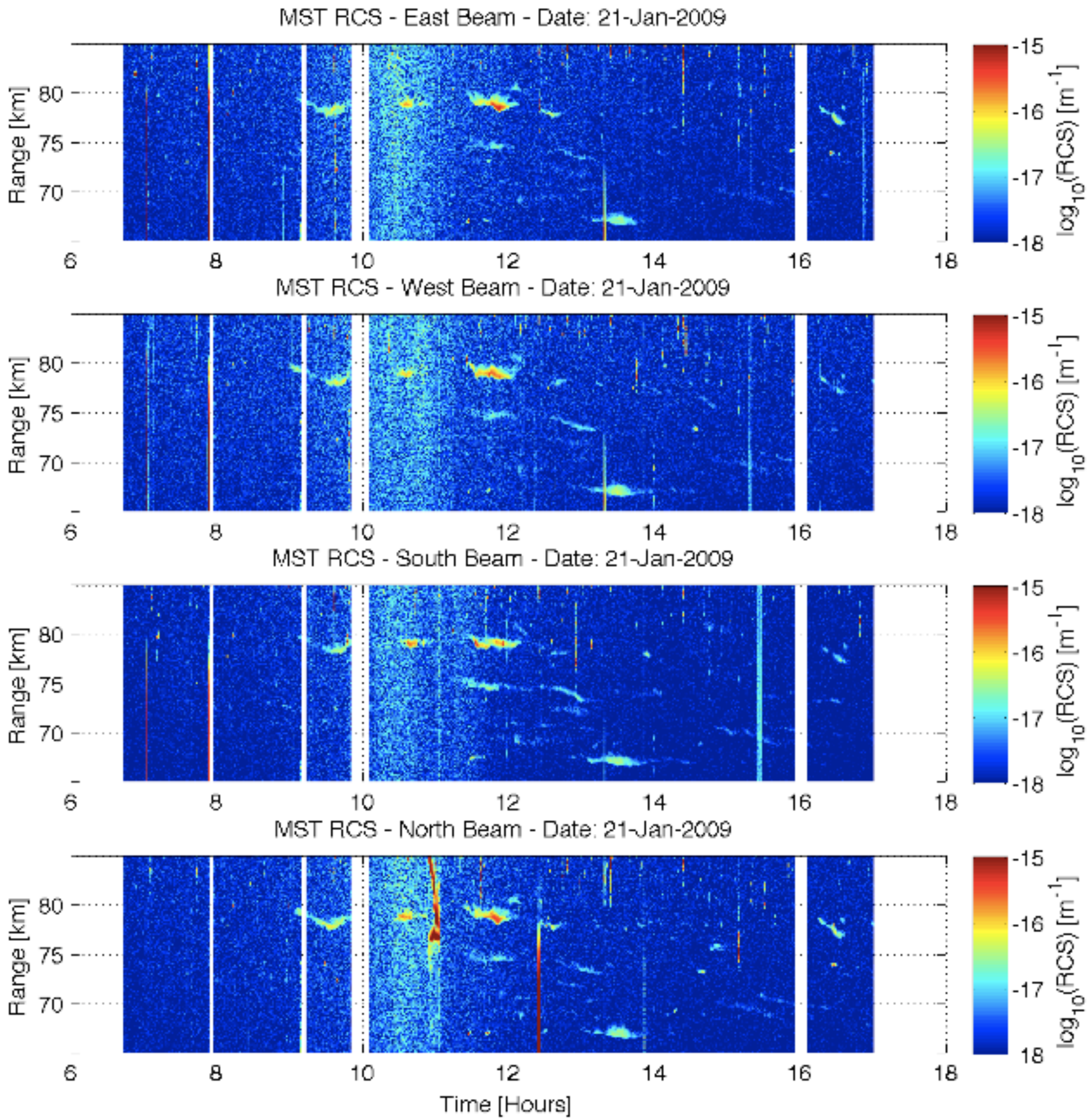
MST RCS - East Beam - Date: 21-Jan-2009
MST RCS - West Beam - Date: 21-Jan-2009
MST RCS - South Beam - Date: 21-Jan-2009
MST RCS - North Beam - Date: 21-Jan-2009
Range [km]
70
75
80
6
8
10
12
14
16
18
Time [Hours]
log10(RCS) [m-1]
-15
-16
-17
-18

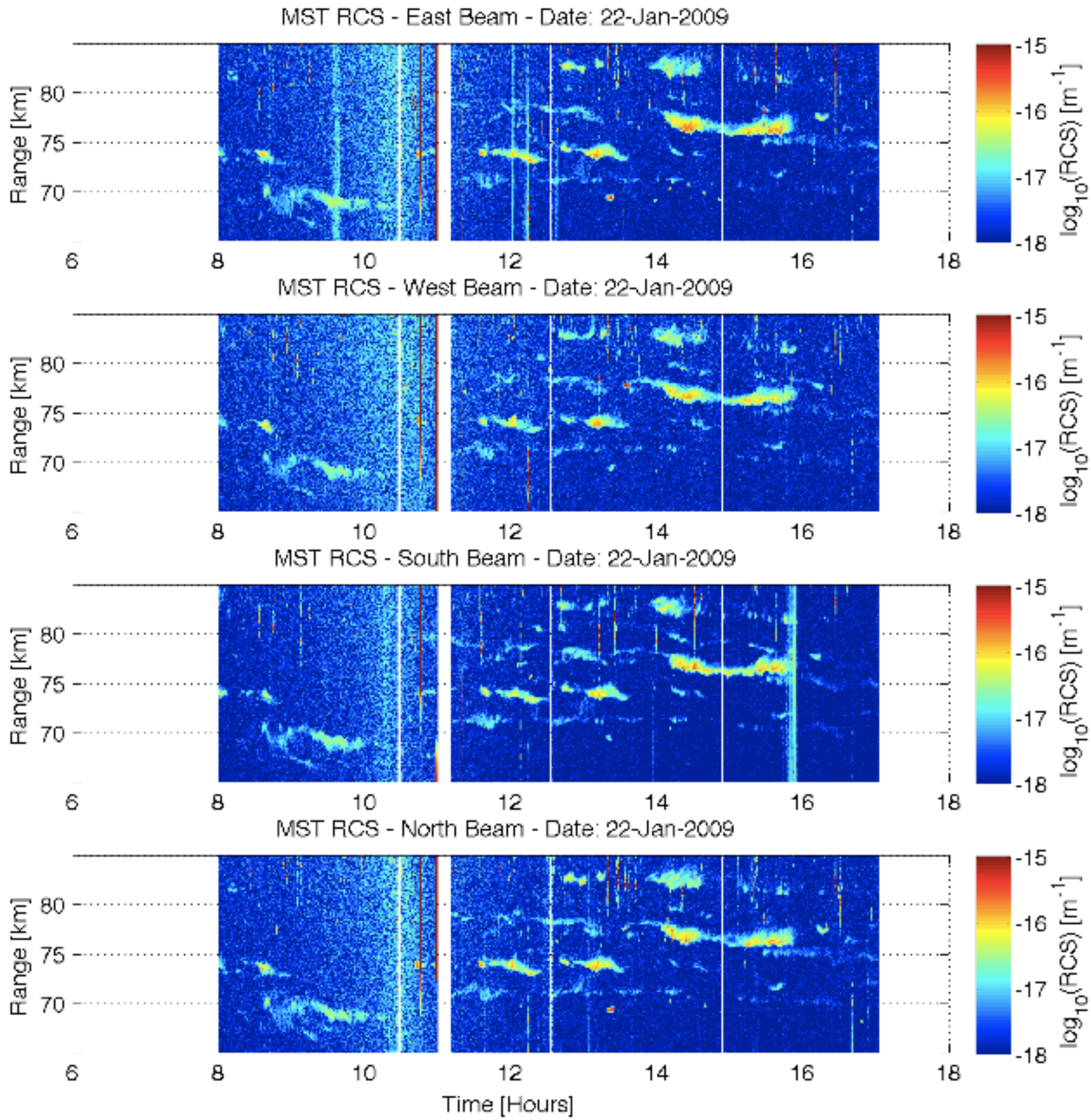
MST RCS - East Beam - Date: 22-Jan-2009
MST RCS - West Beam - Date: 22-Jan-2009
MST RCS - South Beam - Date: 22-Jan-2009
MST RCS - North Beam - Date: 22-Jan-2009
Range [km]
70
75
80
6
8
10
12
14
16
18
Time [Hours]
-15
-16
-17
-18
log10(RCS) [m-1]

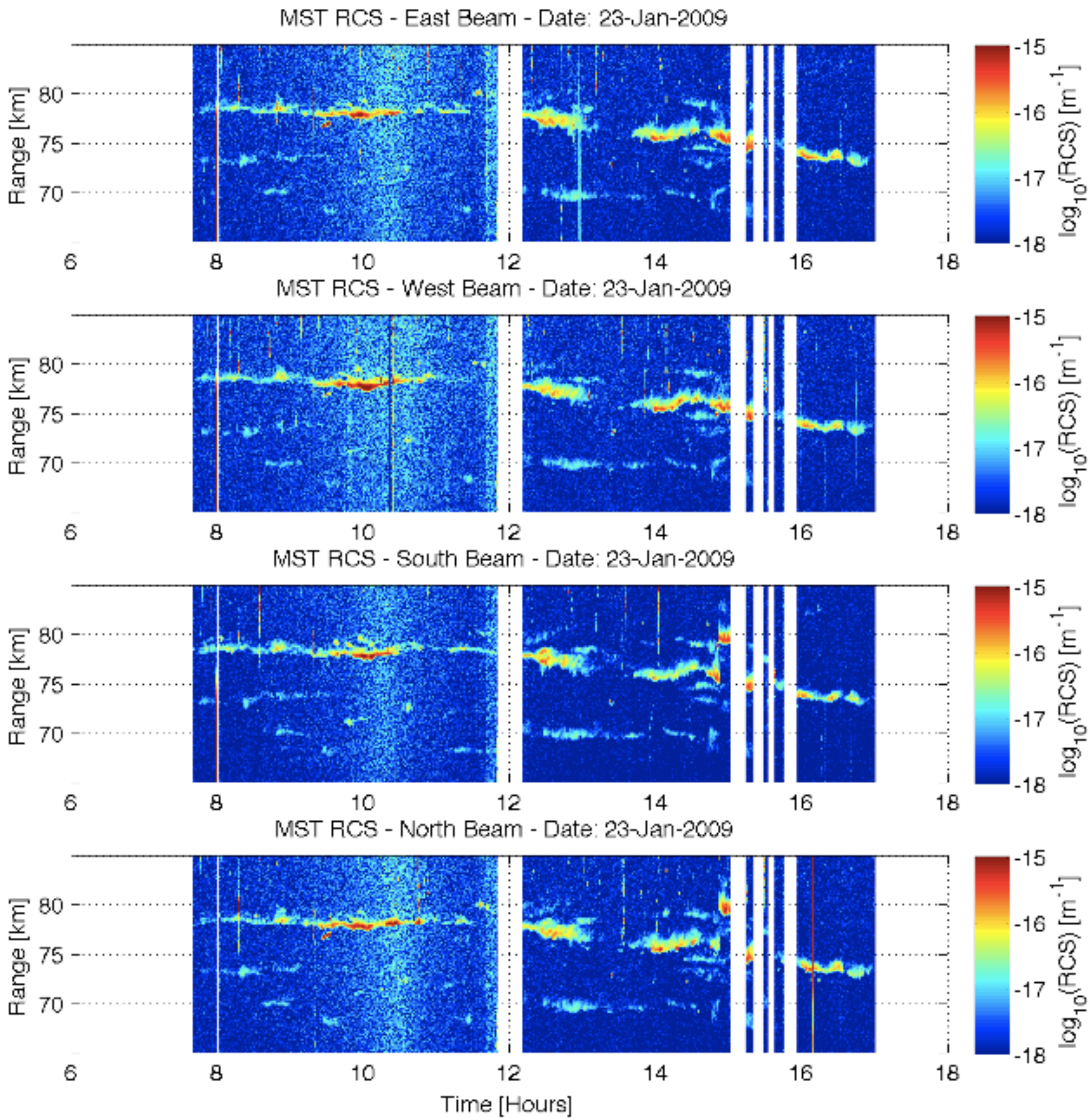

MST RCS - East Beam - Date: 23-Jan-2009
MST RCS - West Beam - Date: 23-Jan-2009
MST RCS - South Beam - Date: 23-Jan-2009
MST RCS - North Beam - Date: 23-Jan-2009
Range [km]
Time [Hours]
log10(RCS) [m-1]

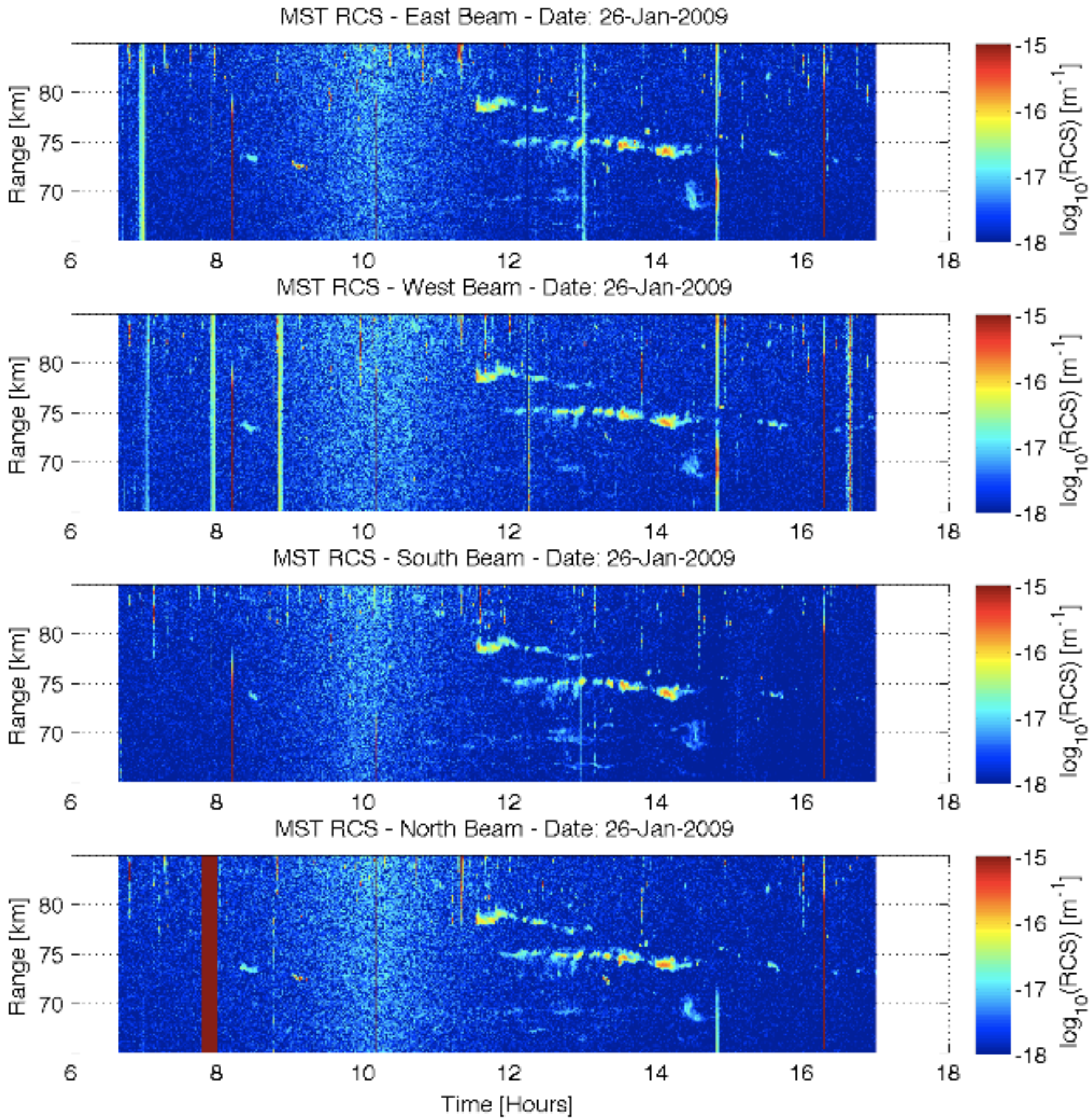

MST RCS - East Beam - Date: 26-Jan-2009
MST RCS - West Beam - Date: 26-Jan-2009
MST RCS - South Beam - Date: 26-Jan-2009
MST RCS - North Beam - Date: 26-Jan-2009
Range [km]
Time [Hours]
log10(RCS) [m-1]

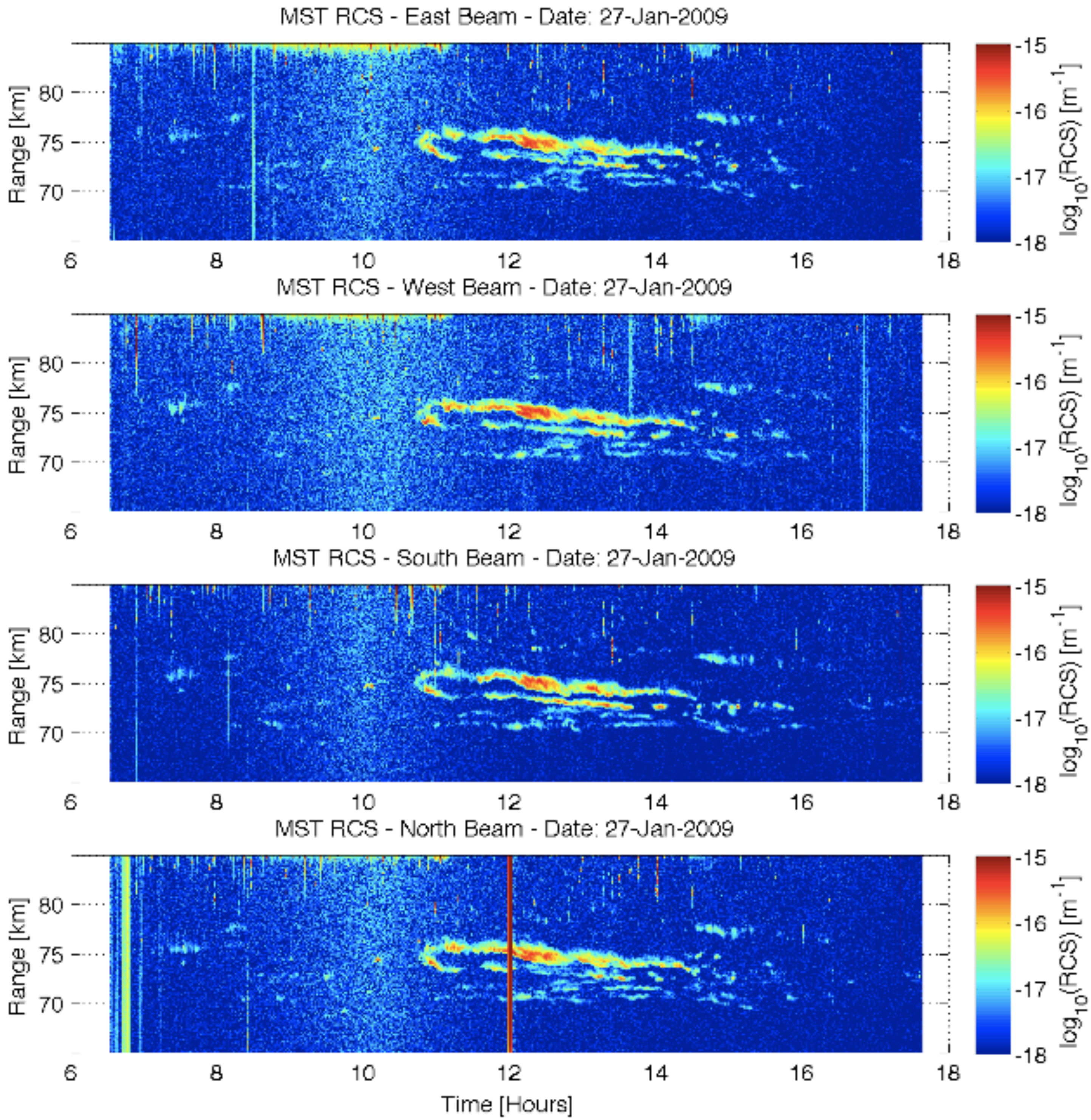
MST RCS - East Beam - Date: 27-Jan-2009
MST RCS - West Beam - Date: 27-Jan-2009
MST RCS - South Beam - Date: 27-Jan-2009
MST RCS - North Beam - Date: 27-Jan-2009
Range [km]
80
75
70
6
8
10
12
14
16
18
Time [Hours]
-15
-16
-17
-18
log10(RCS) [m-1]

Jan 2009: North Beam RCS estimates:

Woodman and Guillen detected 10^-17.3 1/m RCS, close to our detectability threshold at about 10^-18 1/m (using shorter integration and higher resolution than W&G)

We find RCS up to 10^-15 1/m, about 6 orders of magnitude less than PMSE RCS and 3 orders less than winter echoes during solar proton events.

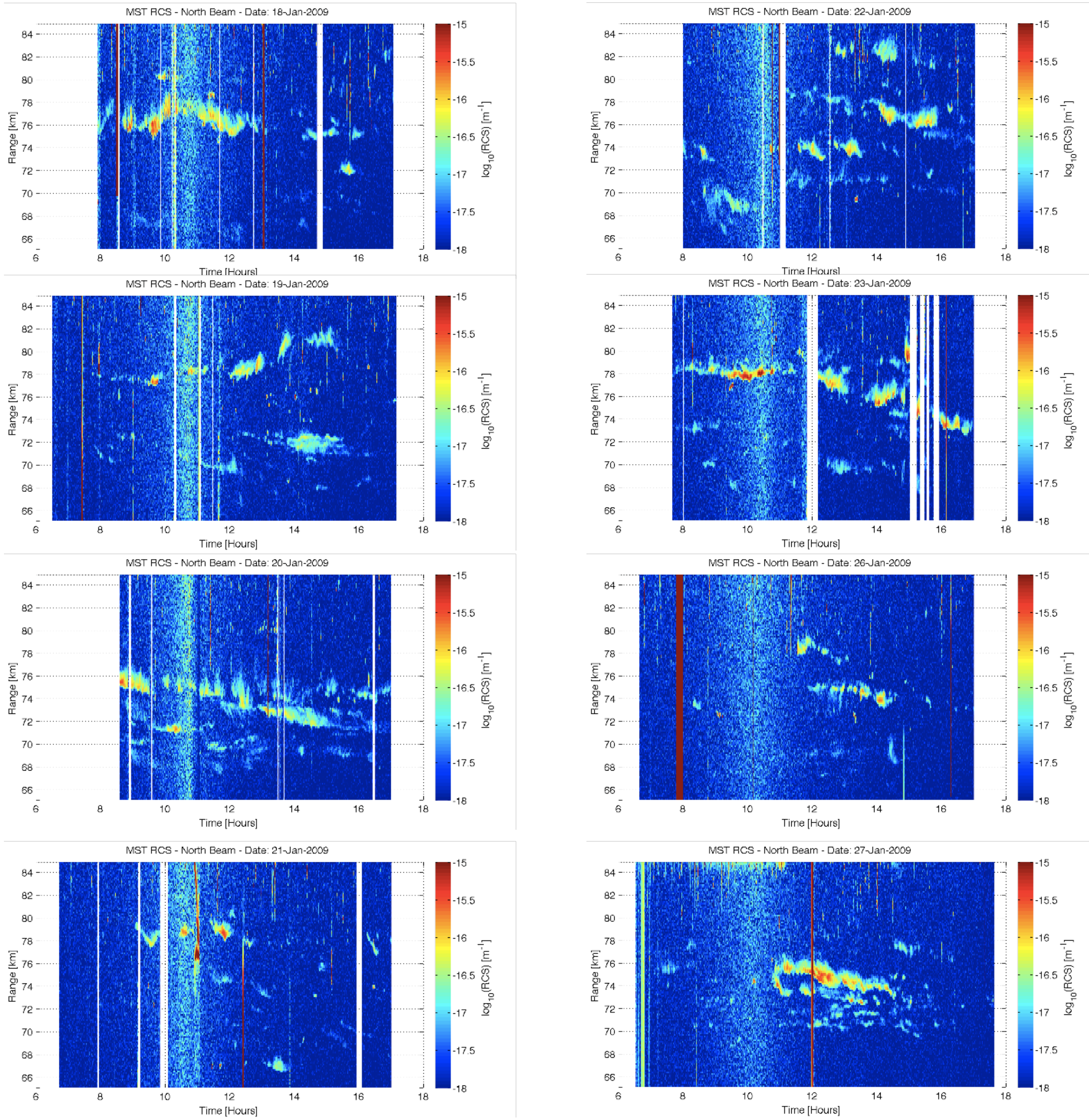

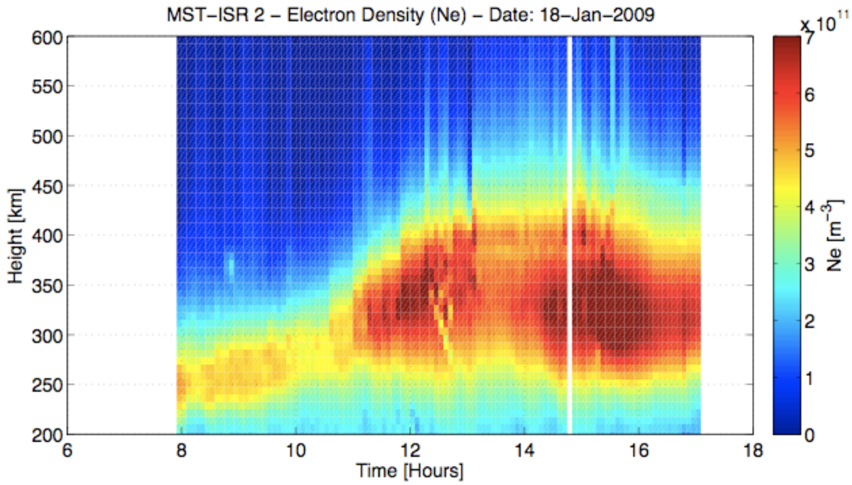
MST–ISR 2 – Electron Density (Ne) – Date: 18–Jan–2009
Height [km]
Time [Hours]
x 10^11
Ne [m^-3]

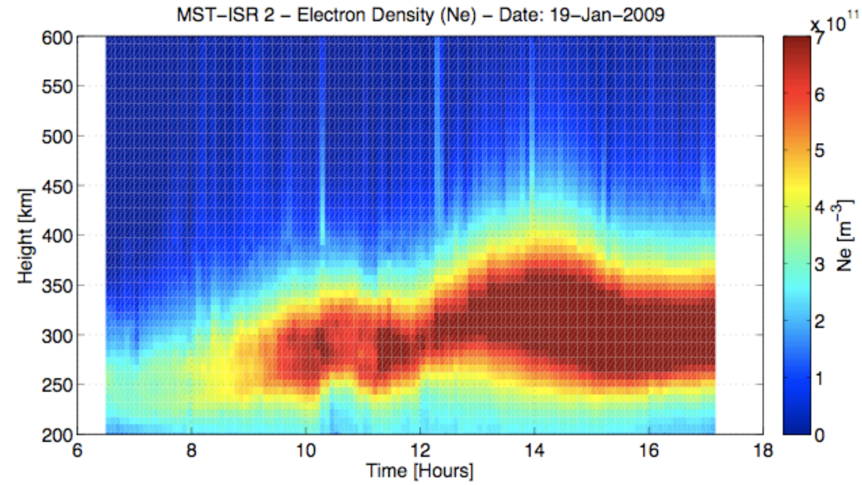
MST–ISR 2 – Electron Density (Ne) – Date: 19–Jan–2009
Height [km]
Time [Hours]
x 10^11
Ne [m^-3]

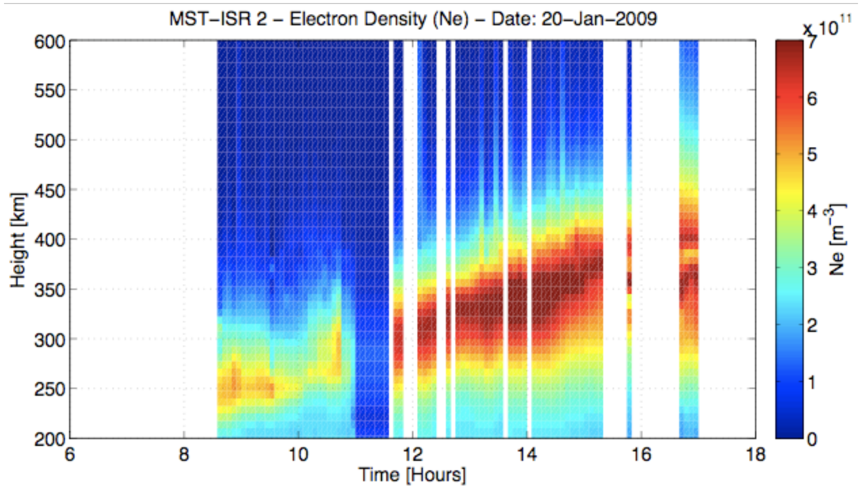
MST–ISR 2 – Electron Density (Ne) – Date: 20–Jan–2009
Height [km]
Time [Hours]
x 10^11
Ne [m^-3]

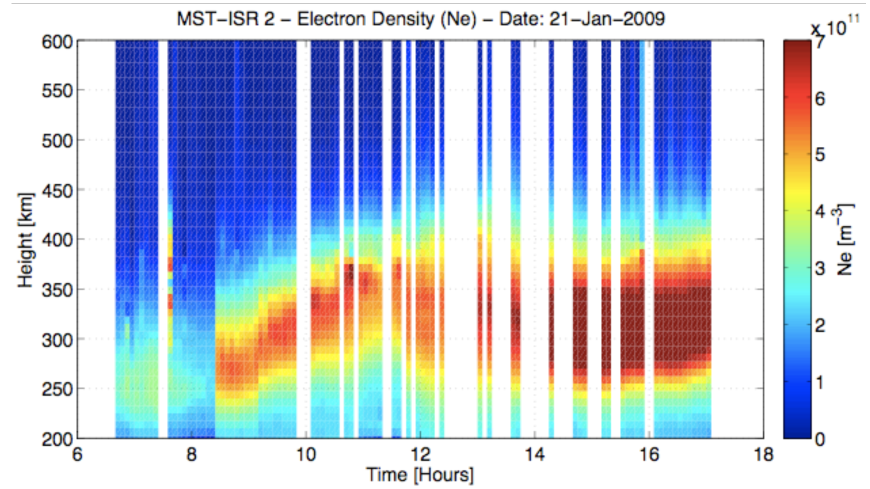
MST–ISR 2 – Electron Density (Ne) – Date: 21–Jan–2009
Height [km]
Time [Hours]
x 10^11
Ne [m^-3]

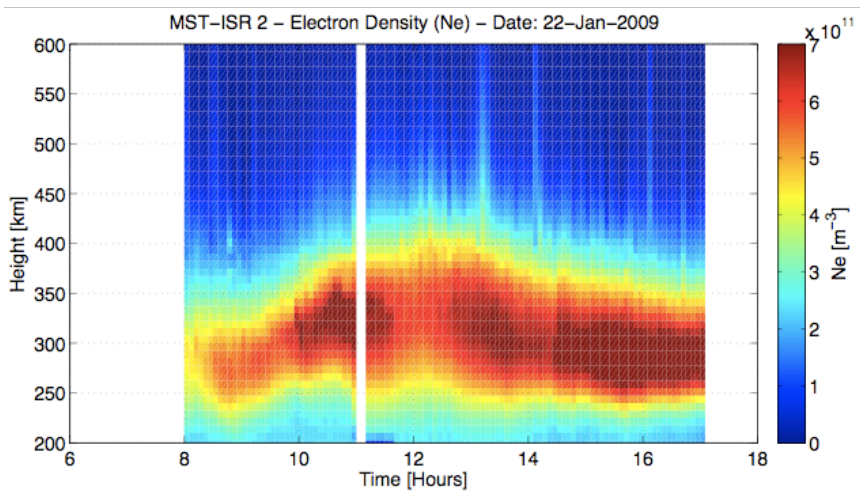
MST–ISR 2 – Electron Density (Ne) – Date: 22–Jan–2009
Height [km]
Time [Hours]
x 10^11
Ne [m^-3]

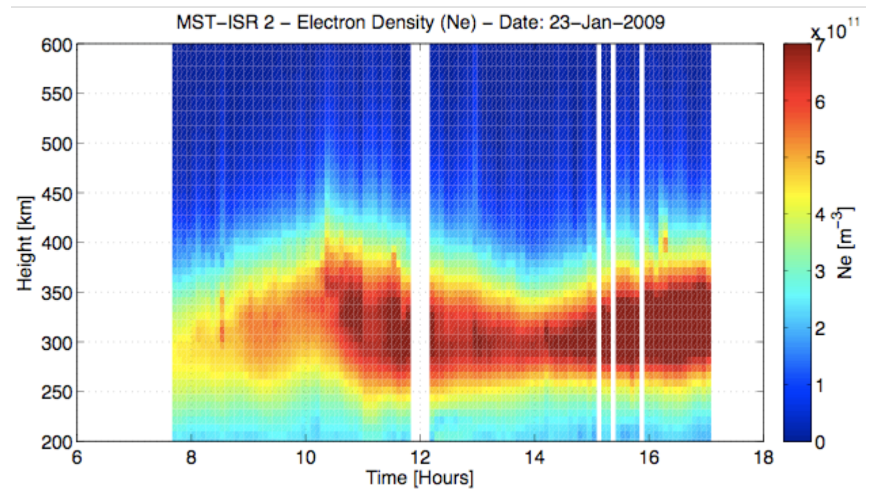
MST–ISR 2 – Electron Density (Ne) – Date: 23–Jan–2009
Height [km]
Time [Hours]
x 10^11
Ne [m^-3]

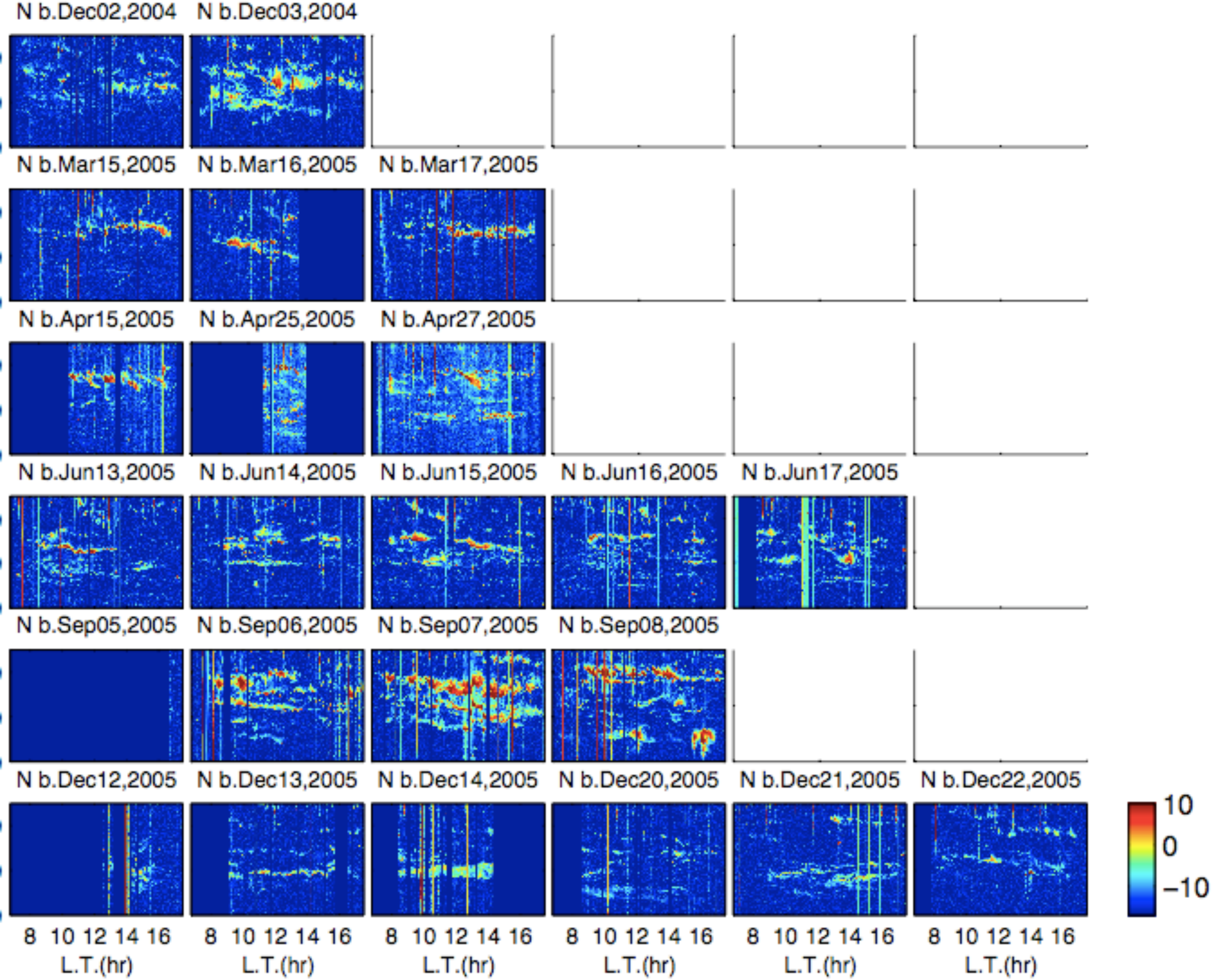
N b.Dec02,2004
N b.Dec03,2004
N b.Mar15,2005
N b.Mar16,2005
N b.Mar17,2005
N b.Apr15,2005
N b.Apr25,2005
N b.Apr27,2005
N b.Jun13,2005
N b.Jun14,2005
N b.Jun15,2005
N b.Jun16,2005
N b.Jun17,2005
N b.Sep05,2005
N b.Sep06,2005
N b.Sep07,2005
N b.Sep08,2005
N b.Dec12,2005
N b.Dec13,2005
N b.Dec14,2005
N b.Dec20,2005
N b.Dec21,2005
N b.Dec22,2005
10
0
−10
8 10 12 14 16
L.T.(hr)

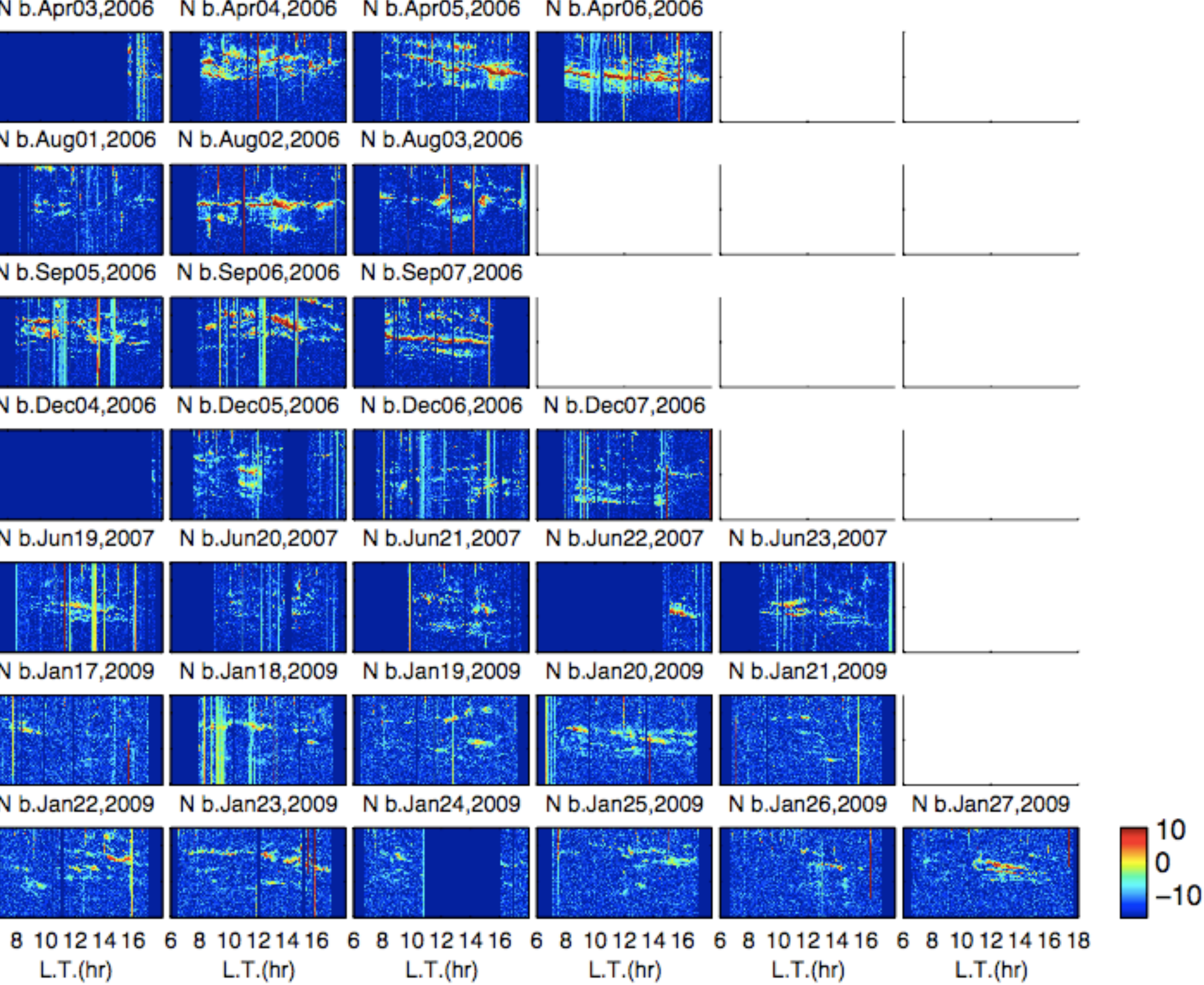

N b.Apr03,2006
N b.Apr04,2006
N b.Apr05,2006
N b.Apr06,2006
b.Aug01,2006
N b.Aug02,2006
N b.Aug03,2006
b.Sep05,2006
N b.Sep06,2006
N b.Sep07,2006
b.Dec04,2006
N b.Dec05,2006
N b.Dec06,2006
N b.Dec07,2006
b.Jun19,2007
N b.Jun20,2007
N b.Jun21,2007
N b.Jun22,2007
N b.Jun23,2007
b.Jan17,2009
N b.Jan18,2009
N b.Jan19,2009
N b.Jan20,2009
N b.Jan21,2009
b.Jan22,2009
N b.Jan23,2009
N b.Jan24,2009
N b.Jan25,2009
N b.Jan26,2009
N b.Jan27,2009
10
0
−10
8 10 12 14 16
6 8 10 12 14 16
6 8 10 12 14 16
6 8 10 12 14 16
6 8 10 12 14 16
6 8 10 12 14 16 18
L.T.(hr)
L.T.(hr)
L.T.(hr)
L.T.(hr)
L.T.(hr)
L.T.(hr)

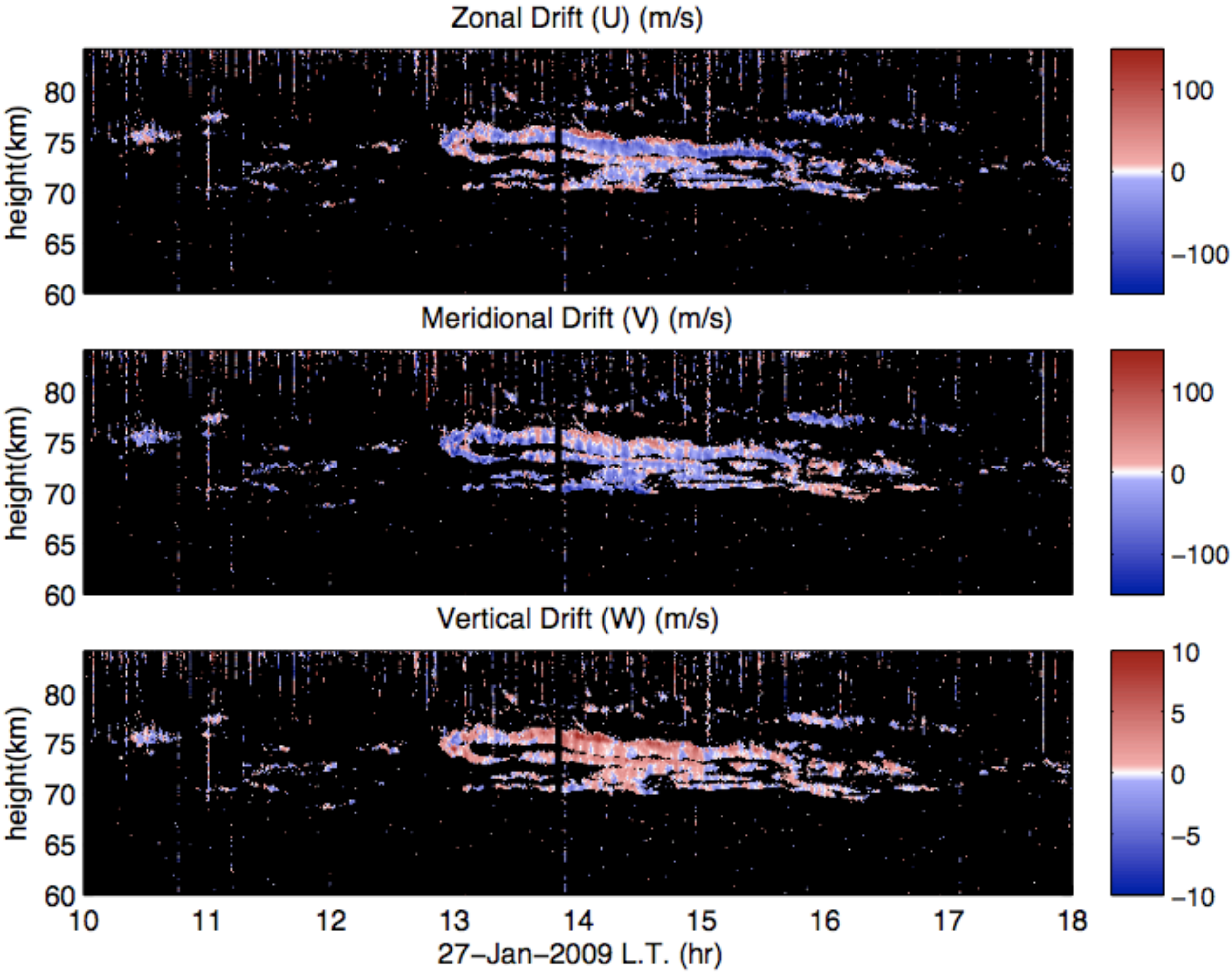

Zonal Drift (U) (m/s)
Meridional Drift (V) (m/s)
Vertical Drift (W) (m/s)
height(km)
60
65
70
75
80
100
0
−100
10
5
−5
−10
10 11 12 13 14 15 16 17 18
27−Jan−2009 L.T. (hr)

Processing the MST region

- MST region sampled range:
  10km - 180km
- pulse compression: Complementary code 64 bauds with flip. Bauds of 150m.
- The 20 contiguous MST pulses are decoded and coherent integrated.
- FFTs of 64 decoded and integrated points separated 133.3ms
- spectra are averaged for 1 minute.

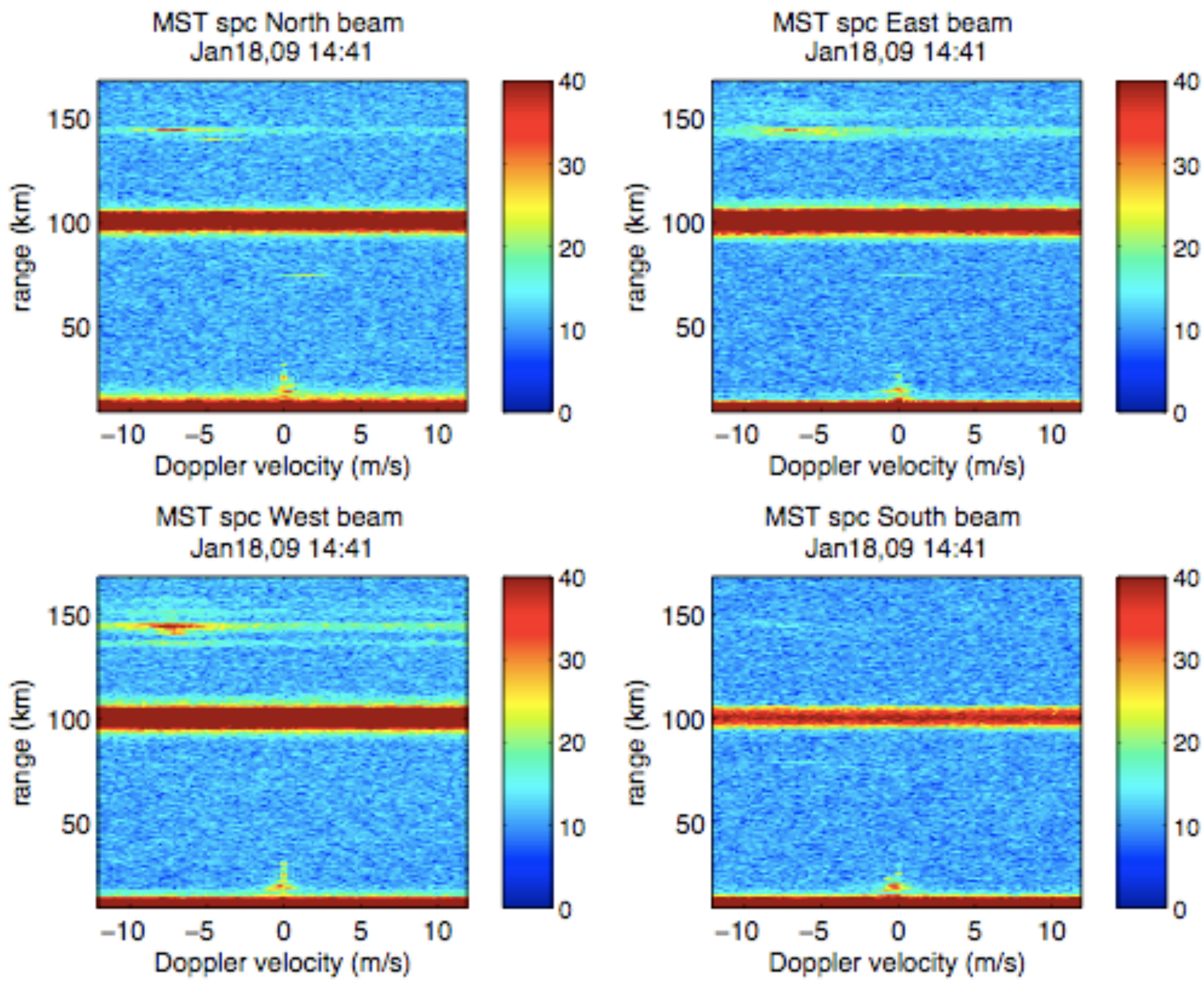

Processing the ISR region

- ISR region sampled range: **75km - 910km**
- pulse compression: **Barker 3** with flip. Baud of 15km.
- The 16 contiguous ISR pulses are decoded and taken the FFT and averaged for 1 minute.
- Spectra cleaned from coherent echoes and atmospheric debris.

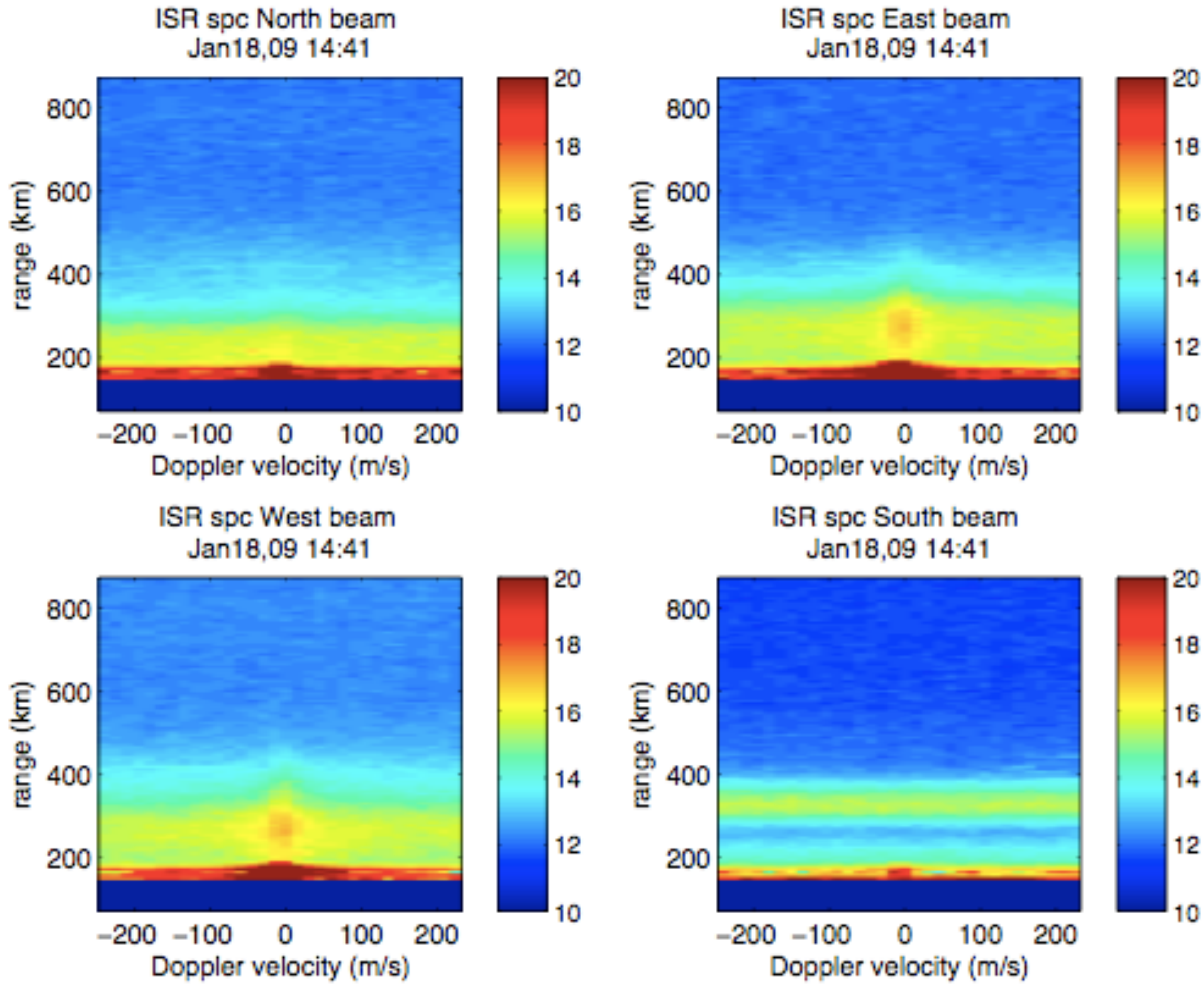

5 minutes averaged Spectra from the 4 beams.

"NEW MST- ISR 2"
Dr's E. Kudeki / J.L.Chau
Jan 2009

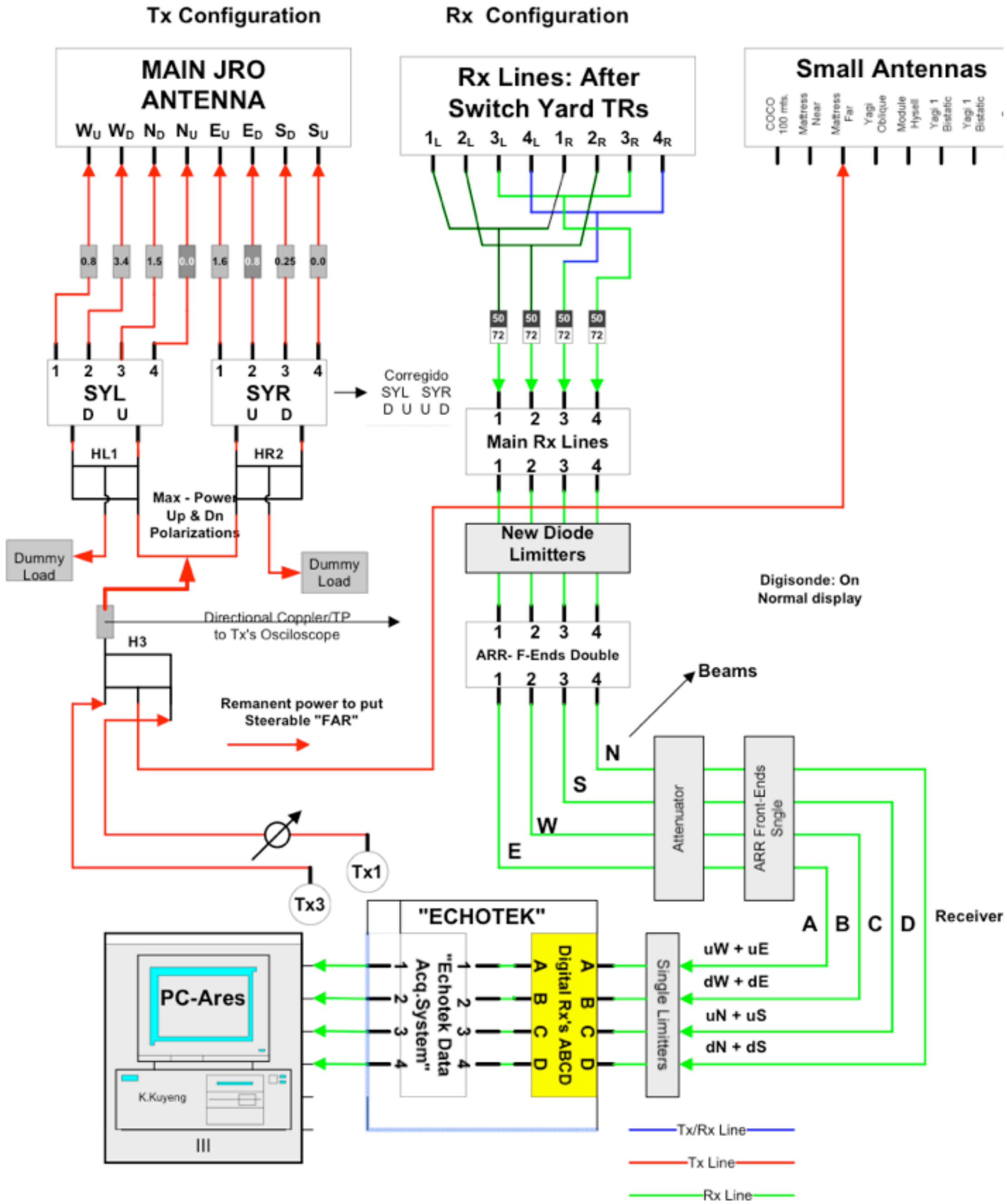

"MST- ISR 2"
Dr's E. Kudeki / J.L.Chau
April:20, 2005 (3 Hybrid mode*)
Jan 2009

Antenna: 4 Beams
Dave Fritts (Original)

North Quarter

4 4.29	5 3.55	2 2.82	3 2.08
5 2.94	2 2.20	3 5.44	4 4.70
2 5.56	3 4.82	4 4.09	5 3.35
3 4.20	4 3.47	5 2.73	2 2.00

East Quarter

2 2	3 5	3 3	3 2
5 3	2 2	2 4	2 3
3 3	4 2	4 4	4 3
2 4	3 3	3 5	3 4

West Quarter

4 4	5 3	5 5	5 4
3 5	4 4	4 2	4 5
5 5	2 4	2 2	2 5
4 2	5 5	5 3	5 2

South Quarter

4 4.29	5 3.55	2 2.82	3 2.08
5 2.94	2 2.20	3 5.44	4 4.70
2 5.56	3 4.82	4 4.09	5 3.35
3 4.20	4 3.47	5 2.73	2 2.00

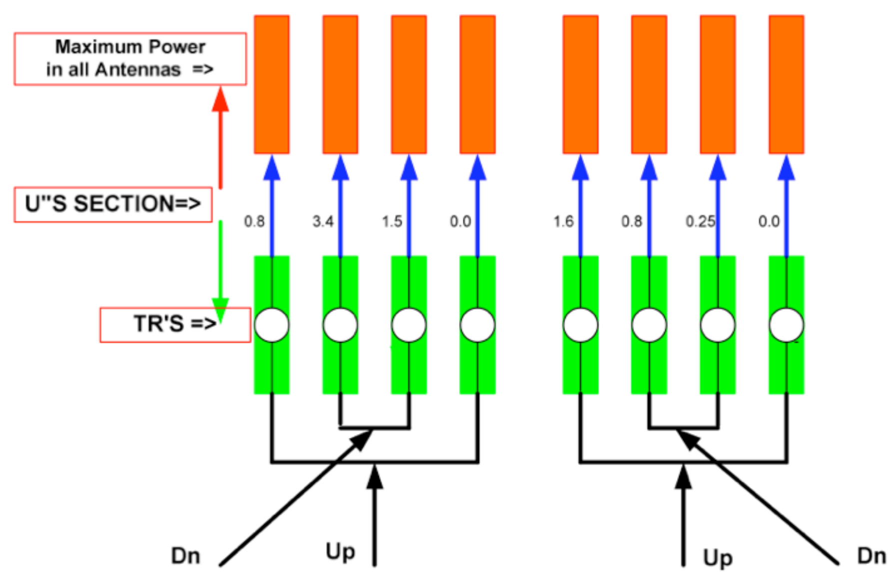

Conclusions

- MST-ISR mode data collected with linearly polarized oblique antennas can be inverted for F-region electron densities, Te/Ti ratios, and channel gain constants.
- During solar-min conditions having ionosonde data is great help --- not essential (still good to have) with higher F-region electron densities.
- Absolute cross-section measurements are useful for beam-to beam and day to day comparisons.
- Multiple-layered vs sparsely layered “days” have been observed to have comparable RCS’s.
- Largest RCS’s are observed in 70-75 km range.
- RCS’s are 6 orders of magnitude weaker than PMSE, and up to 4 orders of magnitude stronger than D-region ISR (typically unobservable at JRO without MST contamination).

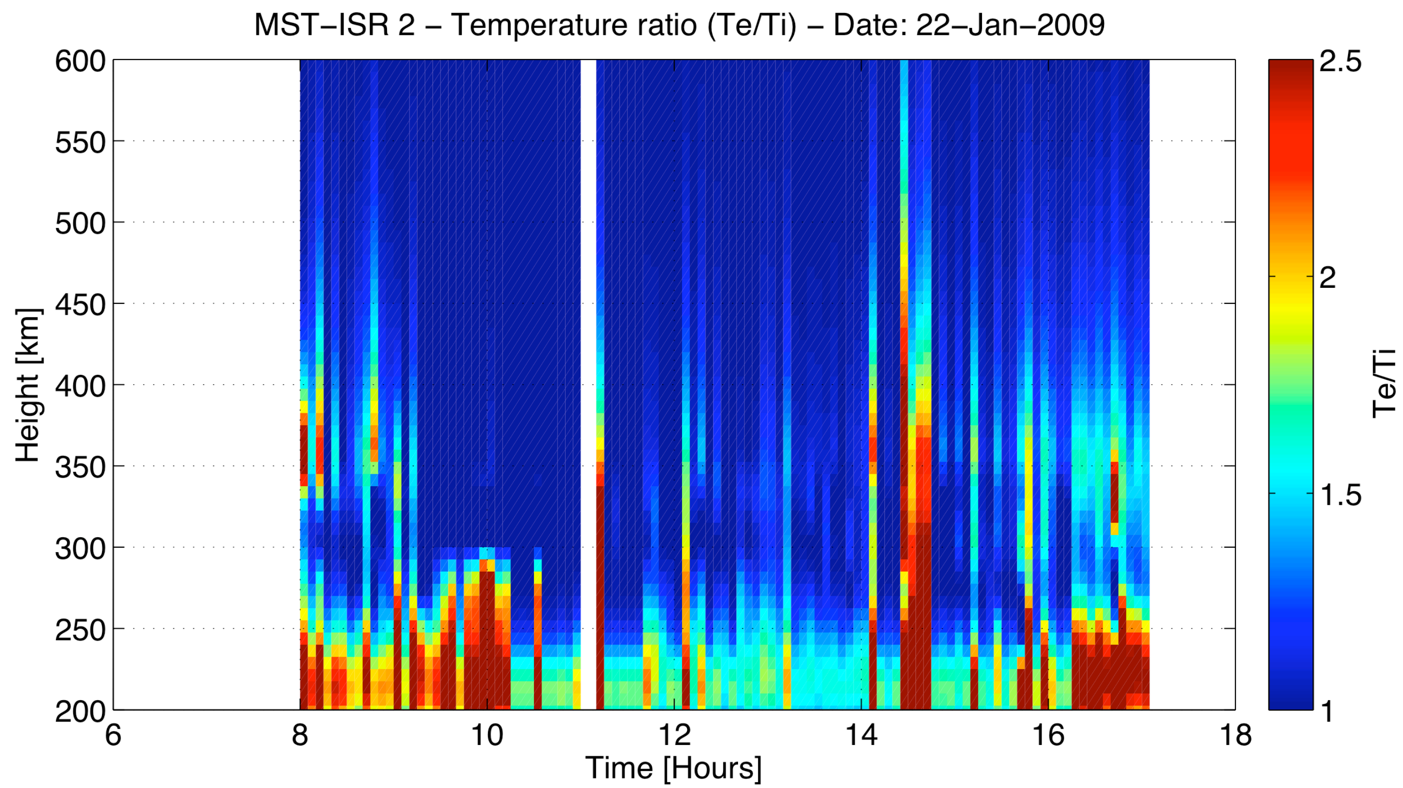

Table 2.1 Radar configuration.

	MST	ISR
Center frequency	49.92 MHz	49.92 MHz
Peak power	1.5 MW	1.5 MW
PCM scheme	64-baud CC	3-baud Barker
Baud length	1 μs	106 μs
Pulse length	64 μs (9.6 km)	318μs (47.7 km)
IPP	200 km	1000 km
Range resolution	150 m	7.95 km
Range	9.6-200 km	75-1000 km
Coherent integrations	20	0
Incoherent integrations	$\sim$ 23 (1 min)	$\sim$ 23 (1 min)